Supporting Information.

Sila-Ibuprofen

Florian Kleemiss, Aileen Justies, Daniel Duvinage, Patrick Watermann, Eric Ehrke, Kunihisa Sugimoto, Malte Fugel, Lorraine A. Malaspina, Anneke Dittmer, Torsten Kleemiss, Pim Puylaert, Nelly R. King, Anne Staubitz, Thomas M. Tzschentke, Ralf Dringen, Simon Grabowsky, Jens Beckmann

Contents of the Supporting Information

This PDF file includes:

1. Characterization
2. Quantum crystallography
3. Force-field development and molecular-dynamics simulations
4. Averaged non-covalent interaction index (aNCI)
5. Averaged interaction energies
6. Free energy perturbation (FEP) calculations
7. Toxicological investigation
8. Enzyme activity measurements to determine IC_{50} values
9. References to methods and software used in the bonding analysis
10. Captions of other Supporting Information
11. References for Supporting Information

Other Supporting Information for this manuscript include the following:

Movie S1
Data S1 to S4

1.) Characterization

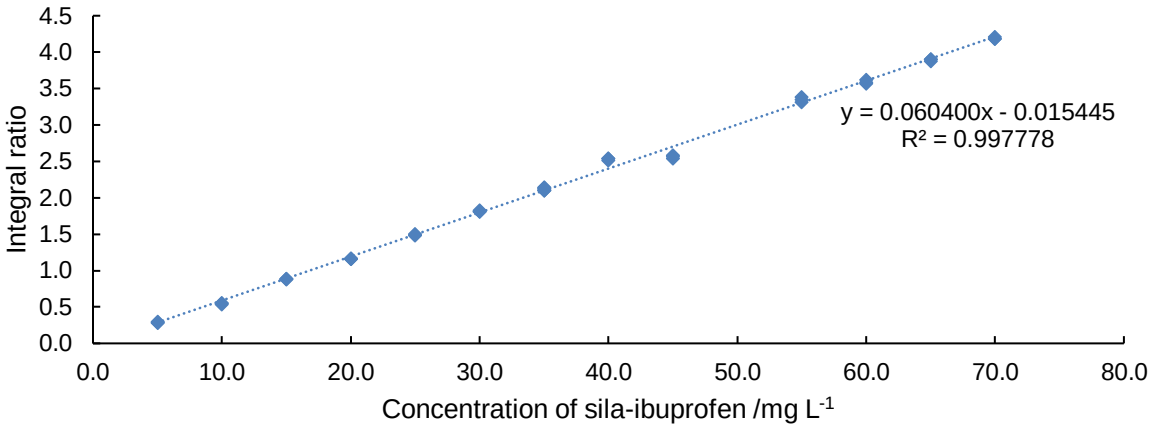

Fig. S1. Calibration curve of the HPLC/UV experiment for the determination of solubility of sila-ibuprofen (**2**) with ibuprofen (**1**) as internal standard. (Value at 50 *mg/L* was discarded due to machine failure)

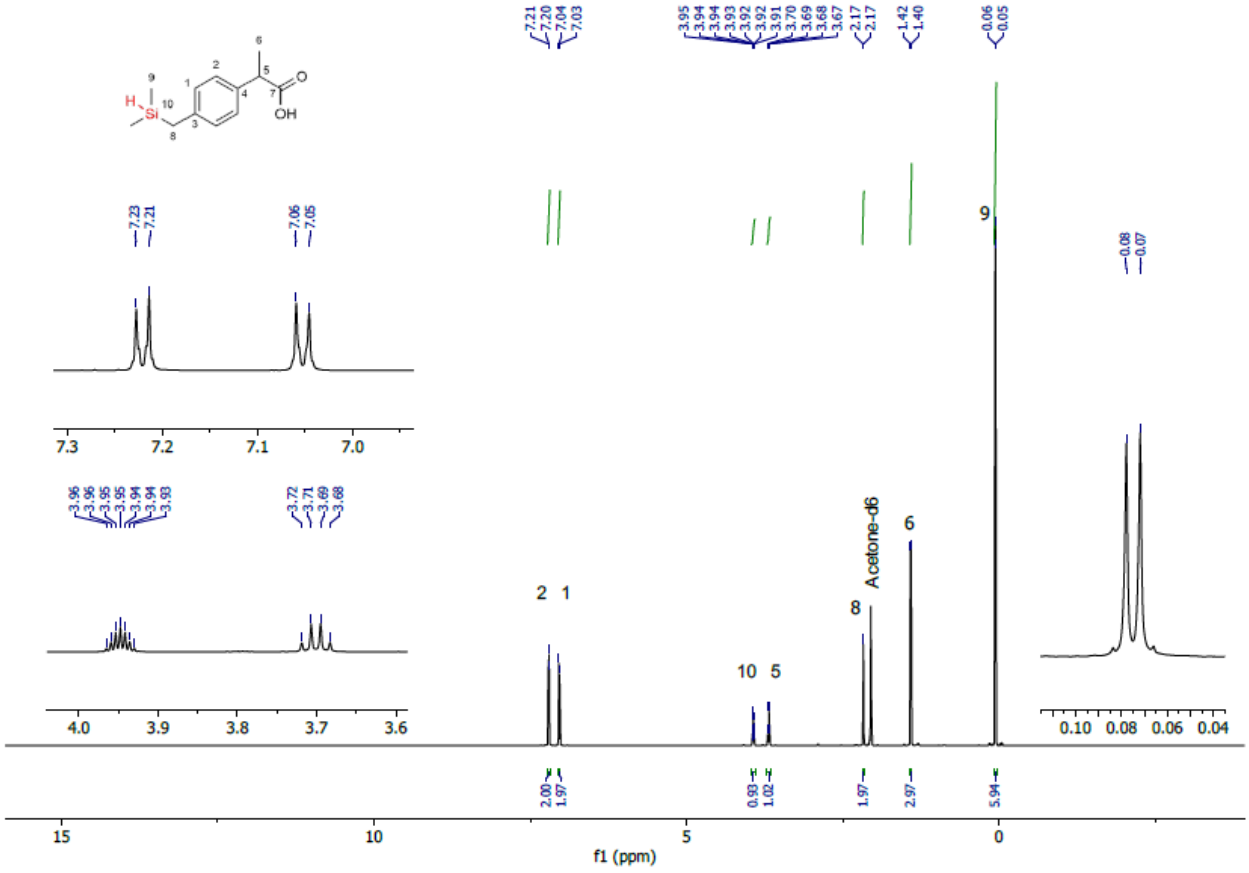

Fig. S2. ^{1}H-NMR spectrum (acetone-d6, 600 MHz) of sila-ibuprofen (**2**).

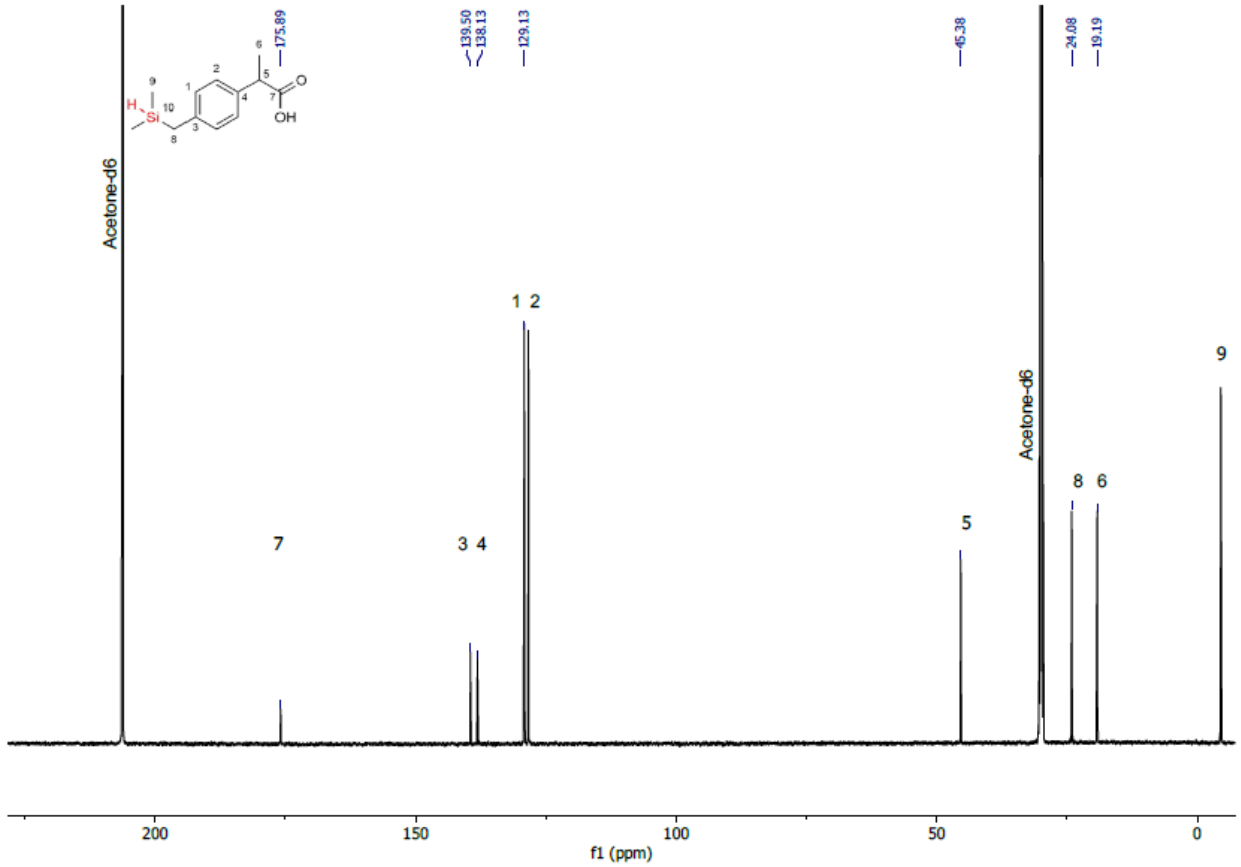

Fig. S3. ^{13}C-{^{1}H}-NMR spectrum (acetone-d6, 151 MHz) of sila-ibuprofen (**2**).

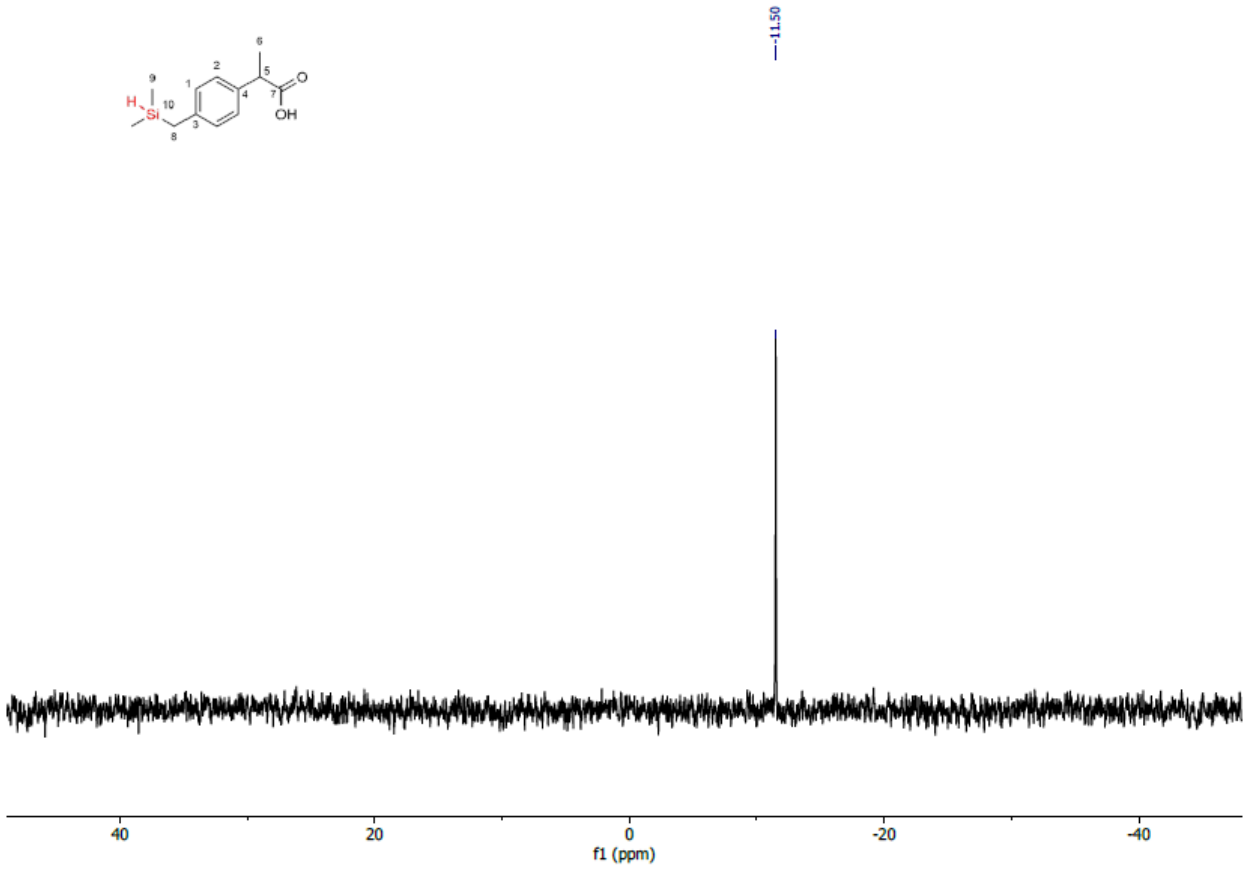

Fig. S4. ^{29}Si-{^{1}H}-NMR spectrum (acetone-d6, 119 MHz) of sila-ibuprofen (**2**).

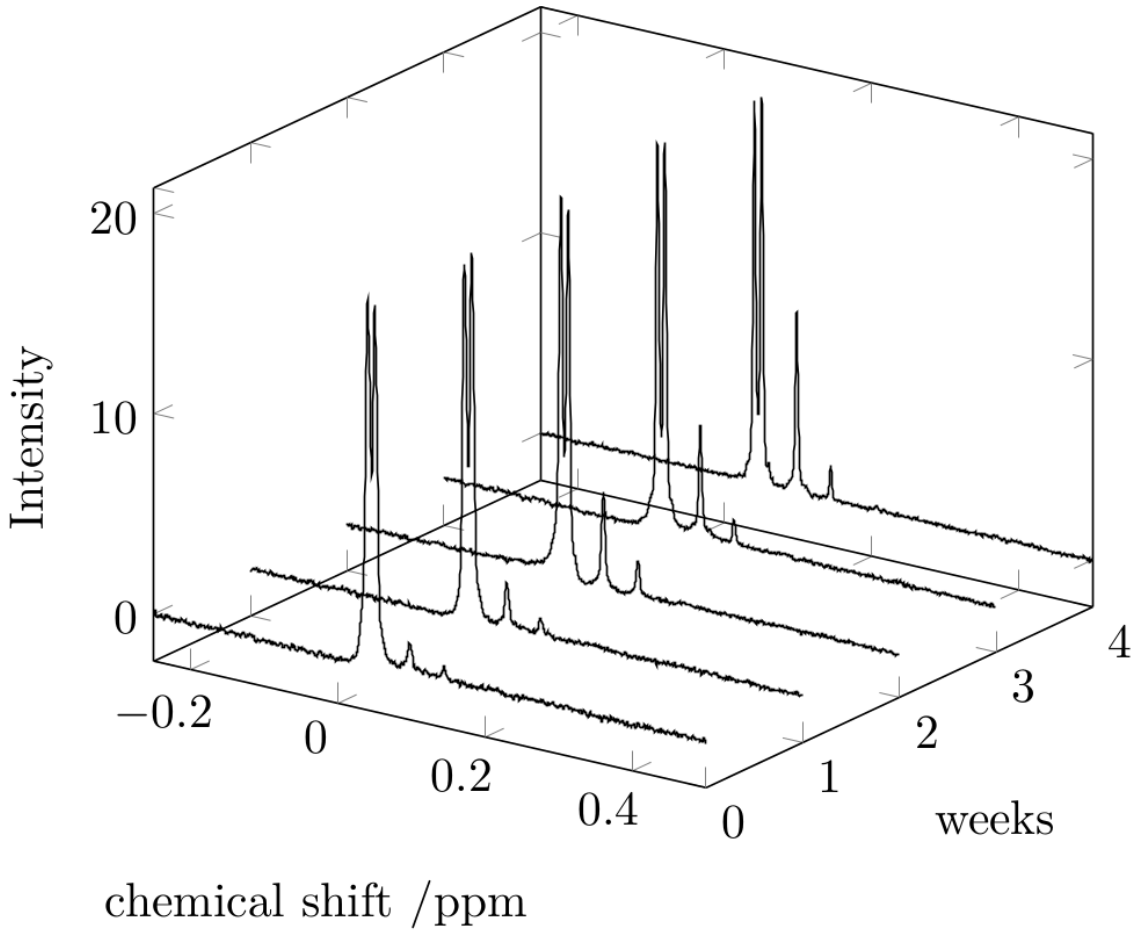

Fig. S5. ^{1}H-NMR spectra of the Me-Si group of sila-ibuprofen (**2**) in a 0.9% NaCl solution, kept at room temperature. Spectra were measured every 7 days. Decomposition is visible after one week.

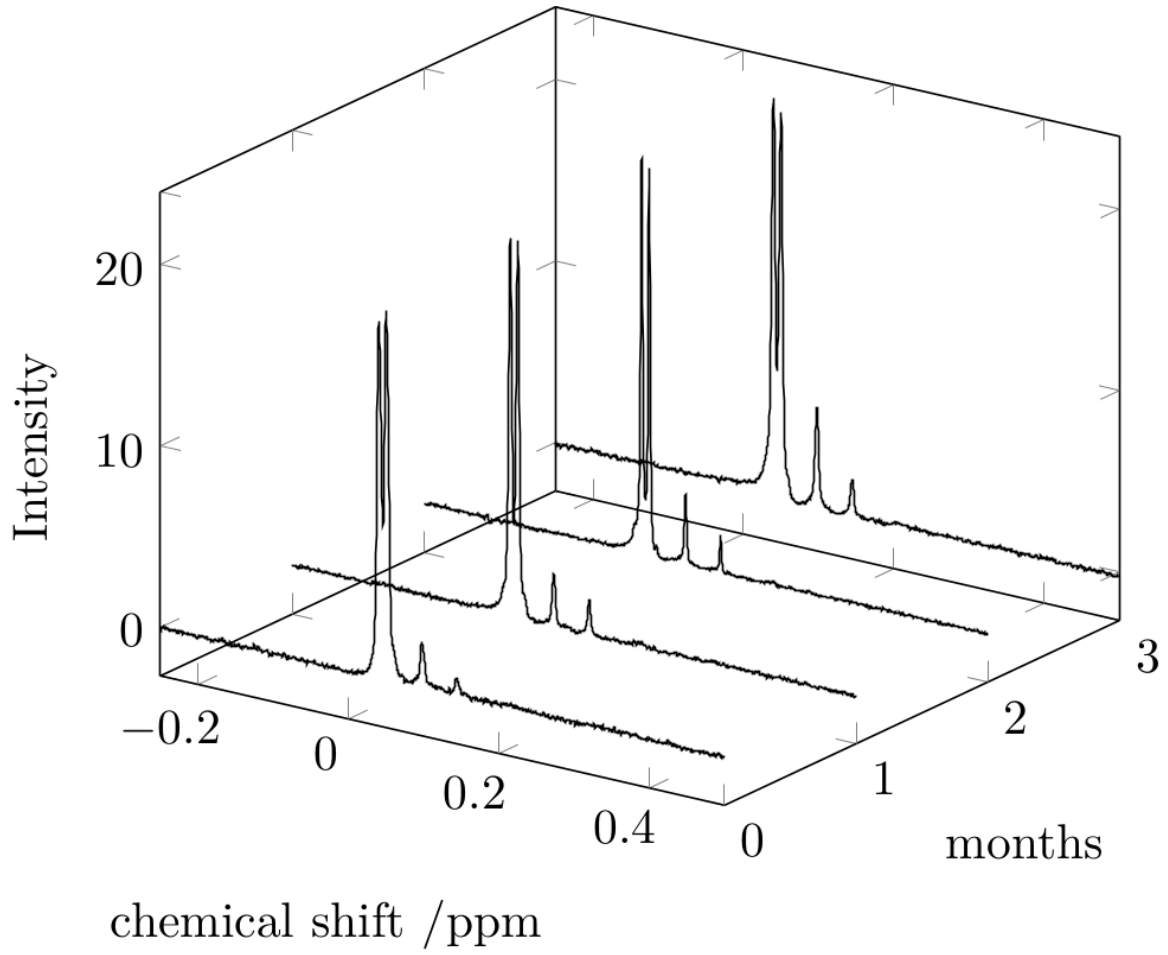

Fig. S6. ^{1}H-NMR spectra of the Me-Si group of sila-ibuprofen (**2**) in a 0.9% NaCl solution, kept at 4°C. Spectra were measured every 28 days. Decomposition is visible after more than a month.

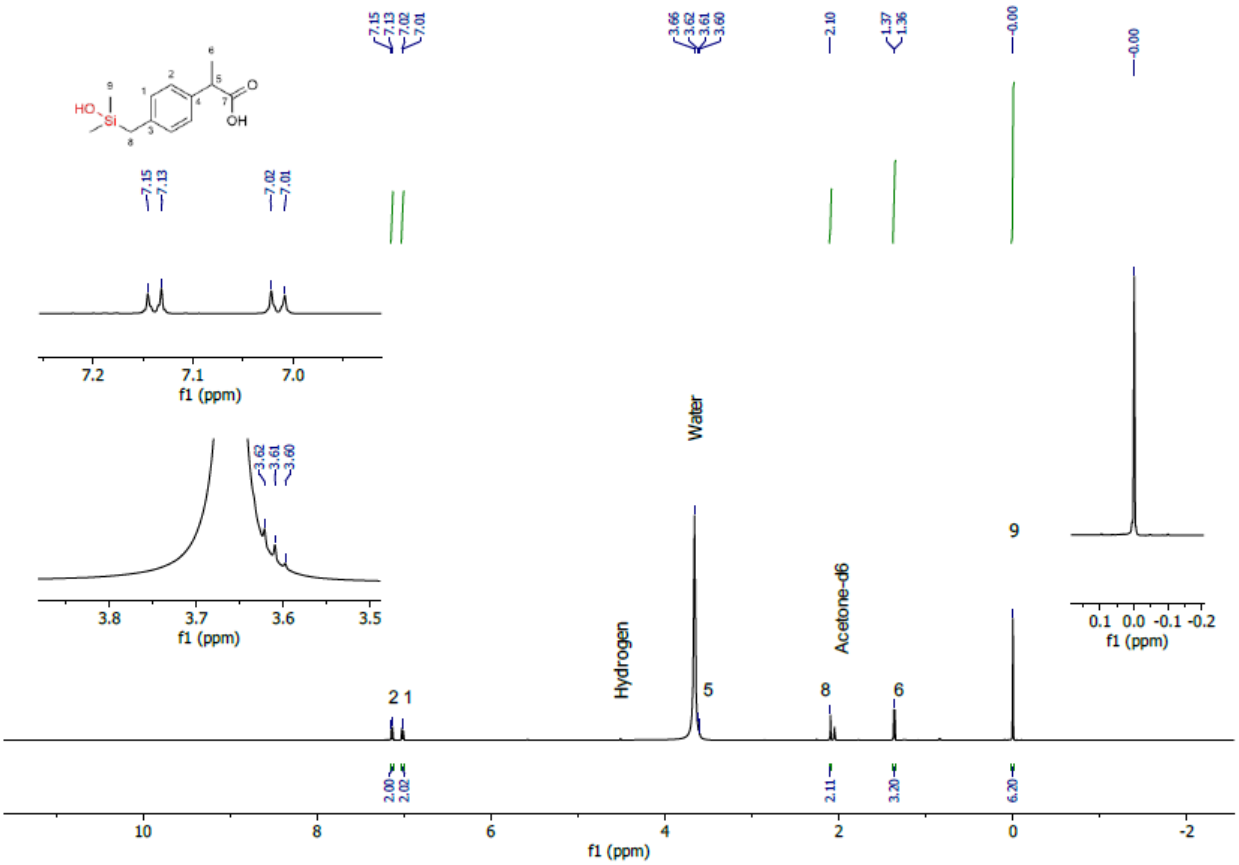

Fig. S7. ^{1}H-NMR spectrum (acetone-d6/water, 600 MHz) of hydroxysila-ibuprofen (**3**) directly from the reaction of sila-ibuprofen (**2**) with Pearlman's catalyst in an acetone-d6 – water mixture.

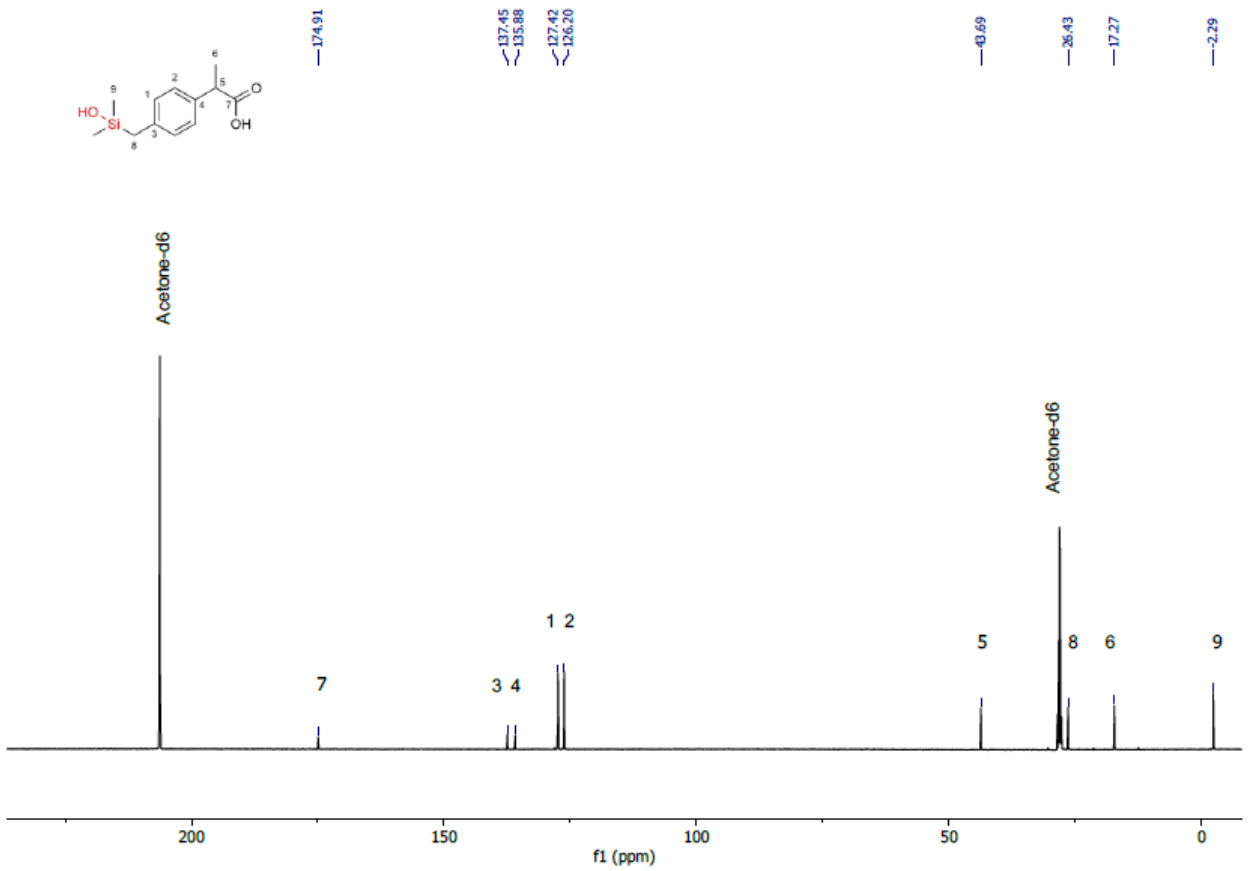

Fig. S8. ^{13}C-{^{1}H}-NMR spectrum (acetone-d6/water, 151 MHz) of hydroxysila-ibuprofen (**3**) directly from the reaction of sila-ibuprofen (**2**) with Pearlman's catalyst in an acetone-d6 – water mixture.

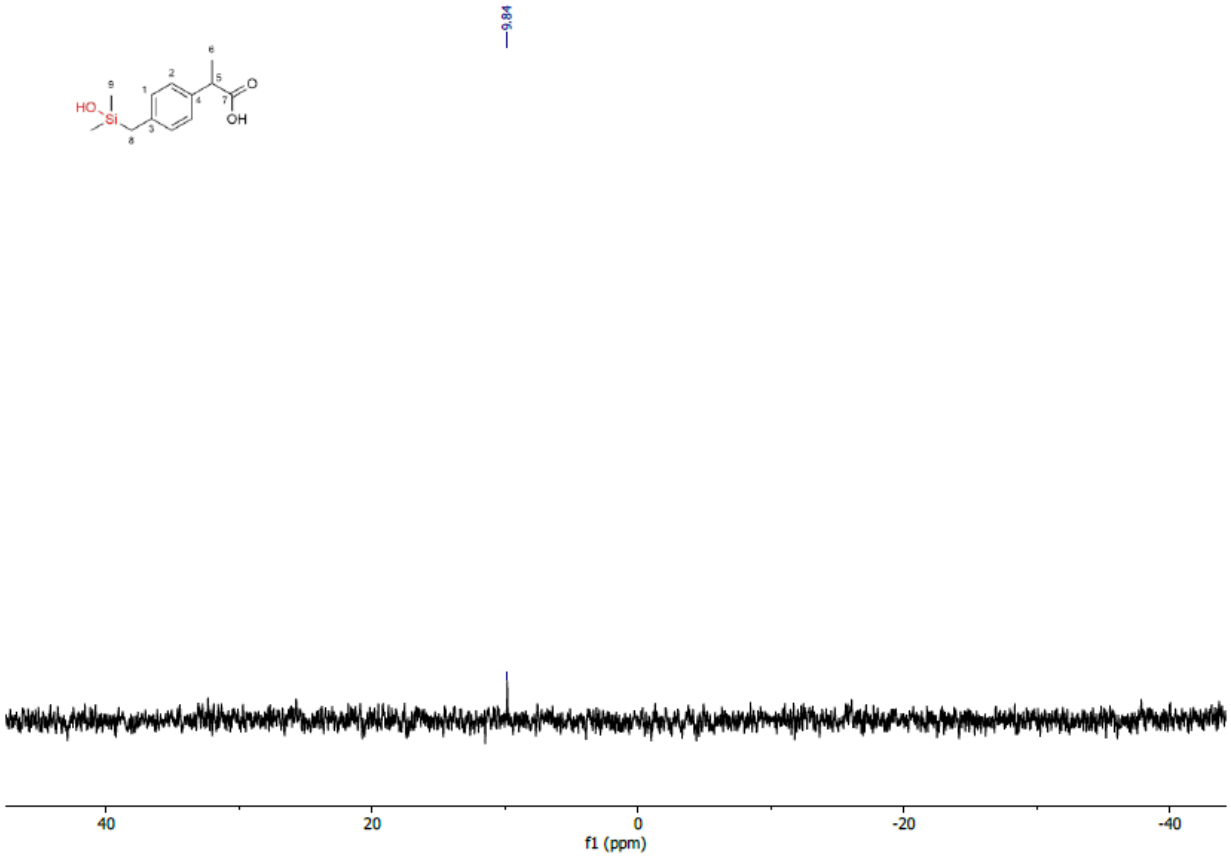

Fig. S9. ^{29}Si-{^{1}H}-NMR spectrum (acetone-d6/water, 119 MHz) of hydroxysila-ibuprofen (**3**) directly from the reaction of sila-ibuprofen (**2**) with Pearlman's catalyst in an acetone-d6 – water mixture.

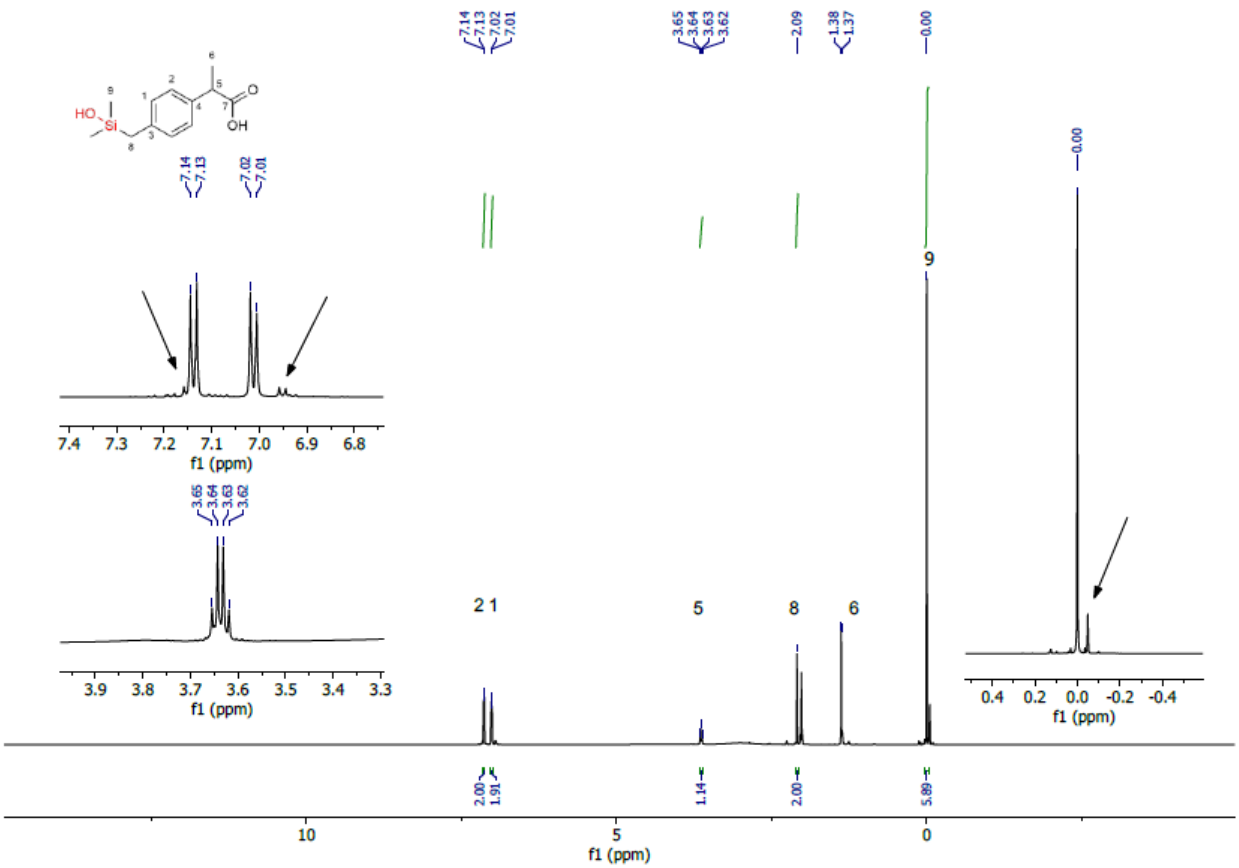

Fig. S10. [1]H-NMR spectrum (acetone-d6, 600 MHz) of hydroxysila-ibuprofen (**3**) after evaporation of the solvent showing condensation to disiloxane (**4**) at room temperature.

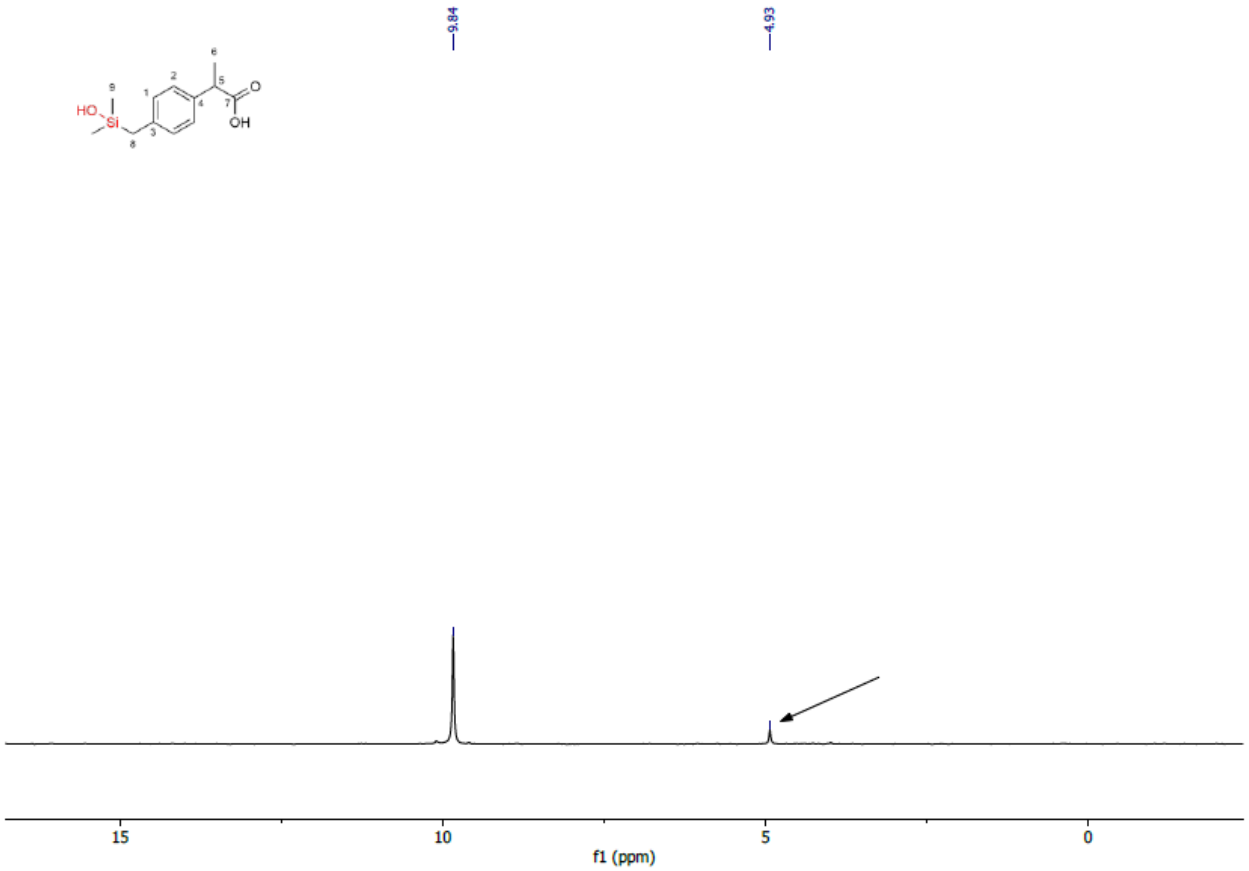

Fig. S11. ^{29}Si-{^{1}H}-NMR spectrum (acetone-d6, 119 MHz) of hydroxysila-ibuprofen (**3**) after evaporation of the solvent showing condensation to disiloxane (**4**).

2.) Quantum crystallography

Table S1. Refinement statistics of XWR for **1** and **2**.

Structure	Ibuprofen (**1**)	Sila-ibuprofen (**2**)
Space group	$P2_1/c$	$P2_1/c$
a /Å	14.465(3)	14.814(3)
b /Å	7.815(2)	7.972(2)
c /Å	10.435(2)	10.798(2)
β /°	99.66(3)	100.70(3)
V /Å^3	1162.9(4)	1253.0(4)
T /K	25	
Resolution /Å	0.45	
Wavelength /Å	0.3567	
R_{int}	0.0552	0.0557
Avg. redundancy	9.49	6.71
Completeness	1.00	1.00
Average I/σ	41.3	22.3
# of refln. measured	132378	105581
# of unique refln.	13367	14320
Criterium for observed refln.	$F_o^2 > 2\sigma(F_o^2)$	
# of observed refln.	10549	10780
Weighting scheme	$w = 1/\sigma(F_o)$	
Final λ	0.40	0.63
Final χ^2	1.7817	2.5273
Final R_1	0.0216	0.0267
Final wR_2	0.0285	0.0365
Max residual density /eÅ^{-3}	0.183	0.261
Min residual density /eÅ^{-3}	-0.139	-0.192
CCDC deposition number	1983628	1983627

Table S2. Full Table of Politzer parameters[14] in $eÅ^{-1}$ or $e^2Å^{-2}$, respectively (V_+: Mean positive values, V_-: Mean negative Values, Π: average deviation from mean value on the surface, σ_+^2,σ_-^2 and σ_{Tot}^2 referring to variance of surface values for positive, negative and all values of the surface, respectively and ν with an upper limit of 0.250 referring to electrostatic balance in interactions of positive and negative regions) for 1 and 2. Calculated using CrystalExplorer.[32]

	Ibuprofen (**1**)	Sila-ibuprofen (**2**)
V_+	0.0217	0.0246
V_-	-0.0306	-0.0302
Π	0.0240	0.0263
σ_+^2	63548	78665
σ_-^2	36953	52630
σ_{Tot}^2	100501	131295
ν	0.2325	0.2401

3.) Force-field development and molecular-dynamics simulations

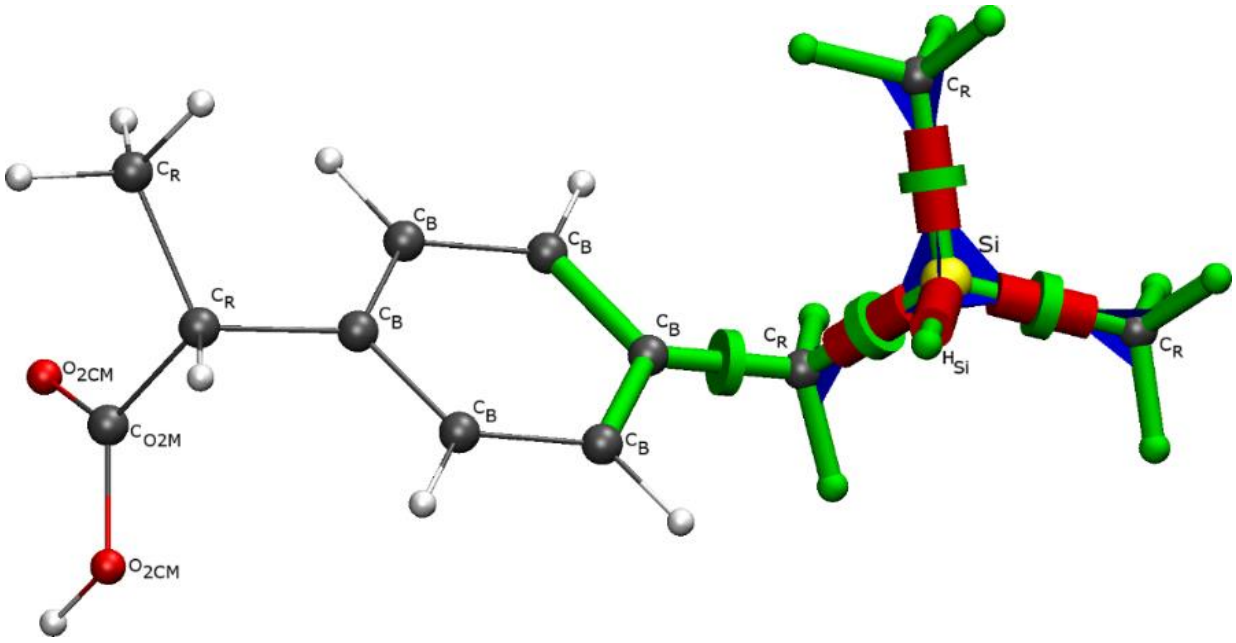

Fig. S12. Visualization of parameters needed to complete the forcefield of **2**. Red cylinders denote missing bond-, blue triangles missing angle- and green discs missing dihedral-parameters. All hydrogen atoms without labels are of type H_{CMM}.

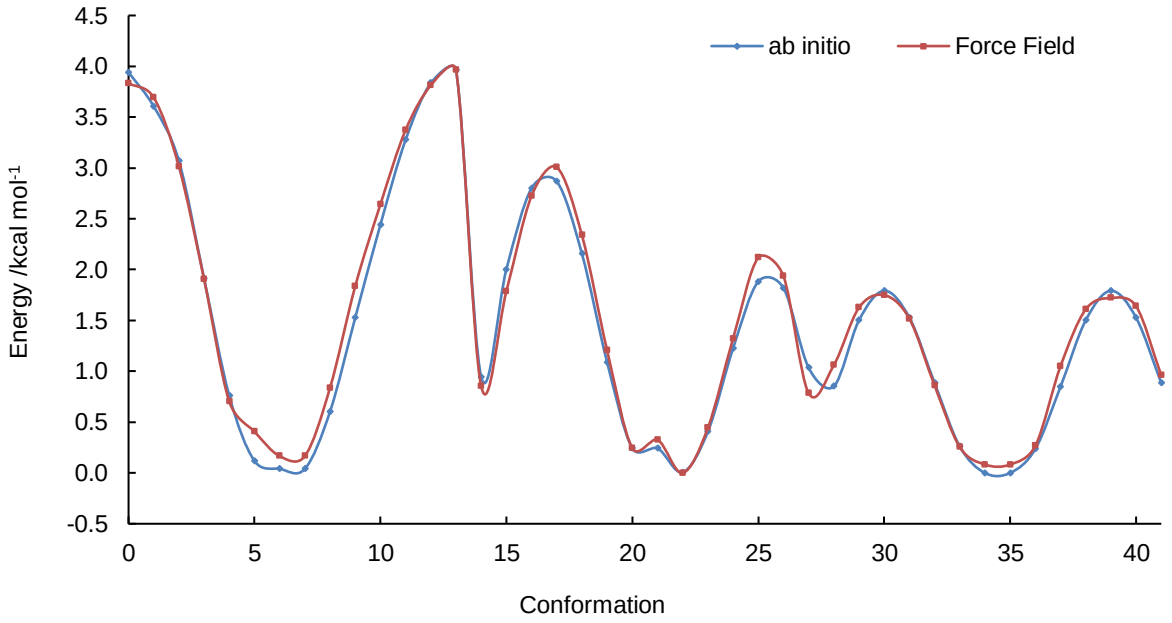

Fig. S13. Plot of the energy comparison between ab initio and force field for the scan around the torsion angles of type C_B-C_B-C_R-Si, C_B-C_R-Si-C_R and H_{CMM}-C_R-Si-H_{Si}.

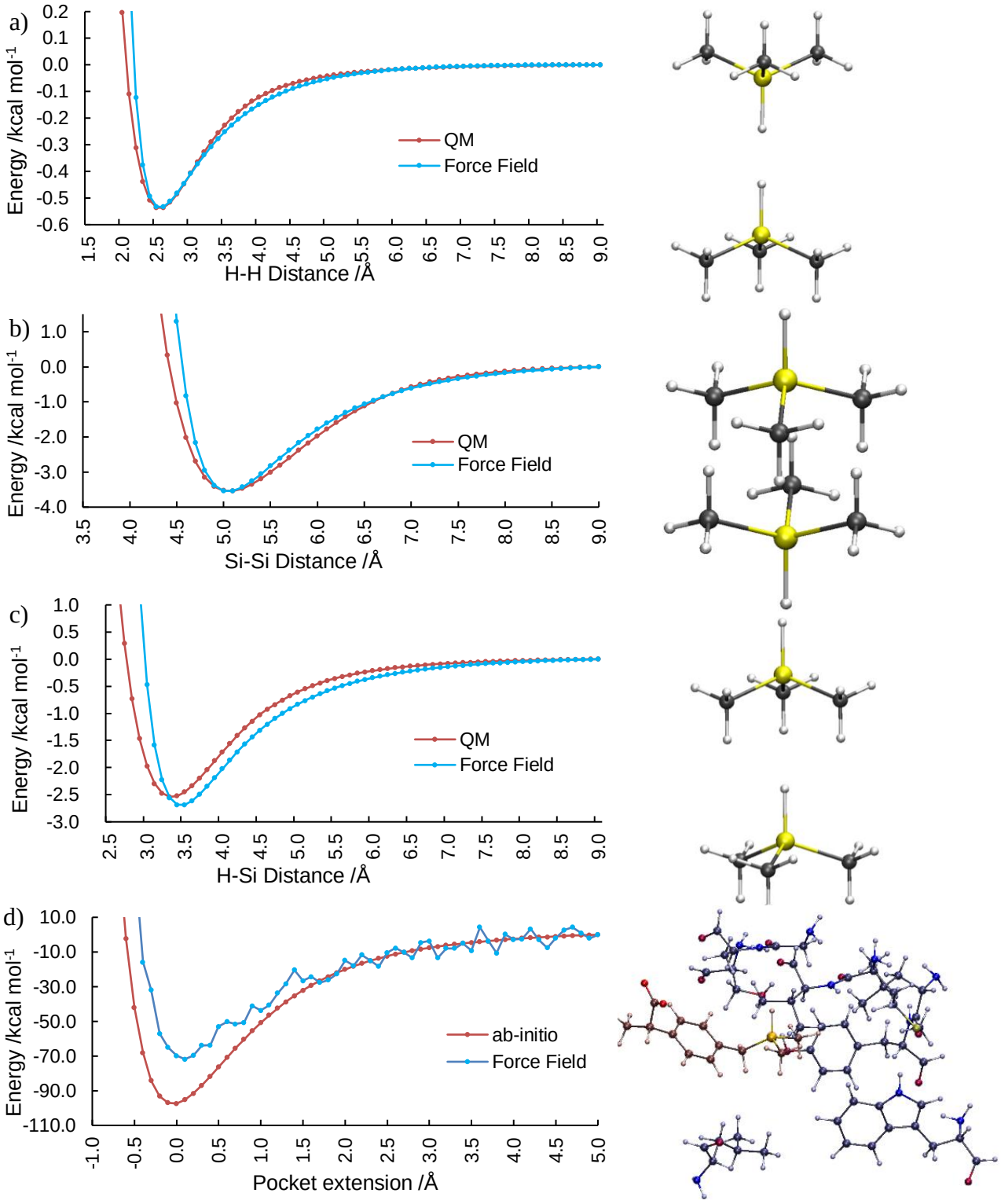

Fig. S14. Comparison of ab initio energies and force field energies for non-bonded interactions in various orientations in a model molecule (a-c) and the active site of the enzyme (d), with color coded sila-ibuprofen (2,red) and amino acids of COX-II (blue).

Table S3.
Parameters of the force field used for **1** and **2** in kcal mol^{-1} Å^{-2} and kcal mol^{-1} rad^{-2}, respectively. The parameters were derived and optimized using the ffTK program.[38]

Parameter (Atoms)	Force constant (K_b, K_θ)	Eq. geometry (b_0, θ_o)	Parameter (Atoms)	Force constant (K_X)	Multiplicity (n)	Eq. geometry (δ)
Bond (C_R Si)	190.6411	1.8677	Dihedral (C_B C_B C_R Si)	0.442	2	180.00
Bond (Si H_{Si})	171.6976	1.4972	Dihedral (C_B C_R Si C_R)	0.331	3	0.00
Bond (C_{O2M} O_{2CM})[a]	702.1030	1.2610	Dihedral (C_B C_R Si H_{Si})	1.091	1	0.00
Bond (C_R C_R)[a]	306.4320	1.5080	Dihedral (C_R Si C_R H_{CMM})	0.000	3	0.00
Bond (C_R H_{CMM})[a]	342.9910	1.0930	Dihedral (H_{CMM} C_R Si H_{Si})	0.301	3	0.00
Bond (C_R C_B)[a]	356.7370	1.4860	Dihedral (C_B C_B C_B C_B)[a]	3.500	2	180.00
Bond (C_R C_{O2CM})[a]	275.6310	1.5100	Dihedral (C_B C_B C_B H_{CMM})[a]	3.500	2	180.00
Bond (C_B C_B)[a]	401.0680	1.3740	Dihedral (C_B C_R C_R H_{CMM})[a]	0.195	3	0.00
Bond (C_B H_{CMM})[a]	381.8530	1.0840	Dihedral (C_B C_R C_{O2M} O_{2CM})[a]	0.300	2	180.00
Angle (C_B C_R Si)	30.2479	105.4005	Dihedral (C_B C_B C_R C_R)[a]	0.225	2	180.00
Angle (C_R Si H_{Si})	22.5564	116.2359	Dihedral (C_B C_B C_R H_{CMM})[a]	-0.210	2	180.00
Angle (C_R Si C_R)	54.1973	114.2112	Dihedral (C_B C_B C_R H_{CMM})[a]	0.196	3	0.00
Angle (Si C_R H_{CMM})	14.9964	110.2184	Dihedral (C_B C_B C_R C_{O2M})[a]	0.100	3	0.00
Angle (C_B C_B C_B)[a]	48.1450	119.9770	Dihedral (C_B C_B C_B C_R)[a]	3.500	2	180.00
Angle (C_B C_B C_R)[a]	57.7880	120.4190	Dihedral (C_B C_R C_R C_R)[a]	0.150	3	0.00
Angle (C_B C_B H_{CMM})[a]	40.5170	120.5710	Dihedral (C_R C_R C_{O2M} O_{2CM})[a]	0.631	2	180.00
Angle (C_R C_R H_{CMM})[a]	45.7700	110.5490	Dihedral (C_R C_B C_B H_{CMM})[a]	3.500	2	180.00
Angle (H_{CMM} C_R H_{CMM})[a]	37.1340	108.8360	Dihedral (H_{CMM} C_R C_R H_{CMM})[a]	0.142	1	0.00
Angle (C_B C_R C_R)[a]	54.4060	108.6170	Dihedral (H_{CMM} C_R C_R H_{CMM})[a]	-0.693	2	180.00
Angle (C_B C_R H_{CMM})[a]	45.1220	109.4910	Dihedral (H_{CMM} C_R C_R H_{CMM})[a]	0.157	3	0.00
Angle (C_B C_R C_{O2M})[a]	71.9660	109.5000	Dihedral (H_{CMM} C_R C_{O2M} O_{2CM})[a]	-0.053	3	0.00
Angle (C_R C_R C_{O2M})[a]	23.7490	98.4220	Dihedral (C_R C_R C_R H_{CMM})[a]	0.320	1	0.00
Angle (H_{CMM} C_R C_{O2M})[a]	37.7820	108.9040	Dihedral (C_R C_R C_R H_{CMM})[a]	-0.315	2	180.00
Angle (C_R C_R C_R)[a]	61.2430	109.6080	Dihedral (C_R C_R C_R H_{CMM})[a]	0.132	3	0.00
Angle (C_R C_{O2M} O_{2CM})[a]	87.0070	114.6890	Dihedral (H_{CMM} C_B C_B H_{CMM})[a]	3.500	2	180.00
Angle (O_{2CM} C_{O2M} O_{2CM})[a]	84.9910	130.6000	Dihedral (C_{O2M} C_R C_R H_{CMM})[a]	-0.070	3	0.00
			Improper (C_B C_B C_B C_R)[a]	2.879	-	-
			Improper (C_B C_B C_B H_{CMM})[a]	1.079	-	-
			Improper (C_B C_R C_B C_B)[a]	2.879	-	-
			Improper (C_{O2M} O_{2CM} C_R O_{2CM})[a]	12.810	-	-

[a]These parameters were taken from swissparam.[28]

Table S4.
Lennard-Jones interaction parameters of the force field.

Atom Type	ε /kcal mol^{-1}	R_{min} /Å
C_B[a]	-0.0700	1.9924
C_R[a]	-0.0550	2.1750
H_{CMM}[a]	-0.0220	1.3200
C_{O2M}[a]	-0.0700	2.0000
O_{2CM}[a]	-0.1200	1.7000
H_{Si}	-0.0152	1.5210
Si	-0.5650	2.3800

[a]These parameters were taken from swissparam.[28]

Table S5.
Charges of atoms in the force field used for **1** and **2**.

Atom Type	Ibuprofen[a] (**1**)	Sila-ibuprofen (**2**)
O_{2CM}	-0.9000	-0.9000
$C_{B,q}$	-0.1435	-0.1435
$C_{B,t}$	-0.1500	-0.1500
C_{02M}	0.9060	0.9060
$C_{R,CH2}$	0.1435	0.1480
$C_{R,CH}$	0.0375	0.0375
$C_{R,CH3-C/Si}$	0.0000	0.0000
H_{CR}	0.0000	0.0000
H_{CB}	0.1500	0.1500
H_{CH}/H_{Si}	0.0000	-0.1470
C_H/*Si*	0.0000	0.1430

[a]These parameters were taken from swissparam.[28]

The most significant difference in the description between **1** and **2** is the assigned charge to the tertiary position where the carbon-silicon-switch was performed. While **1** was described without charges on neither carbon nor hydrogen, as usual in CHARMM force fields,[29] the significant pronunciation of charges observed in the XWR (compare Figure 2) made clear an explicit charge was necessary for **2**.

The parameters in Tables S3 to S5 show not only close resemblance to the quantum mechanically derived energies (compare Figures S5 and S6), but also are in similar orders of magnitude as other parameters used in the CHARMM force field, pointing towards reasonable results of the optimization process.

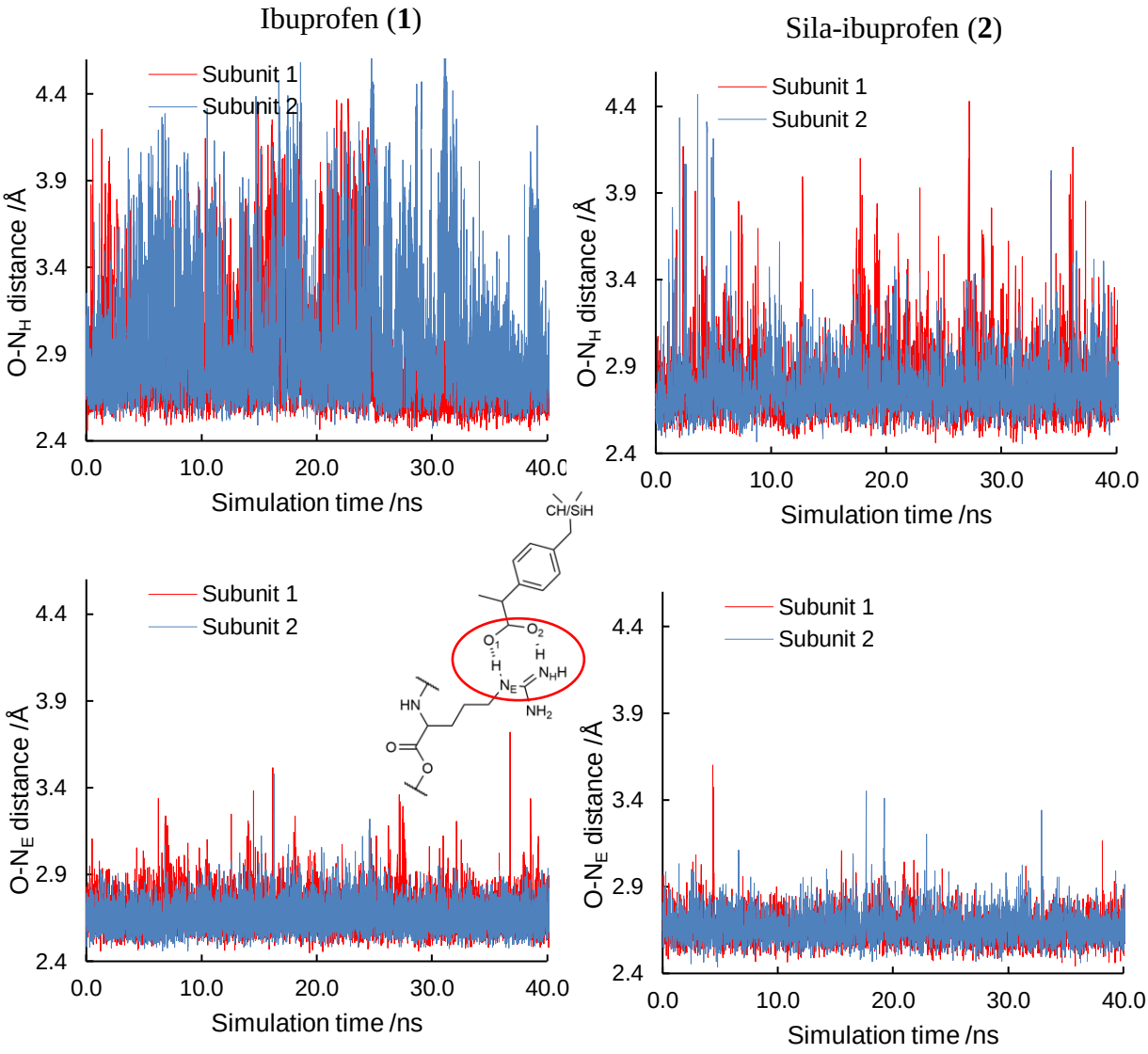

Fig. S15. Plot of arginine-ibuprofen (**1**,left) and -sila-ibuprofen (**2**,right) distances for O_1-N_E and O_2-N_H atoms (in force-field nomenclature, structure shown in figure). There are two subunits in COX-II, which are plotted by color-code (red and blue).

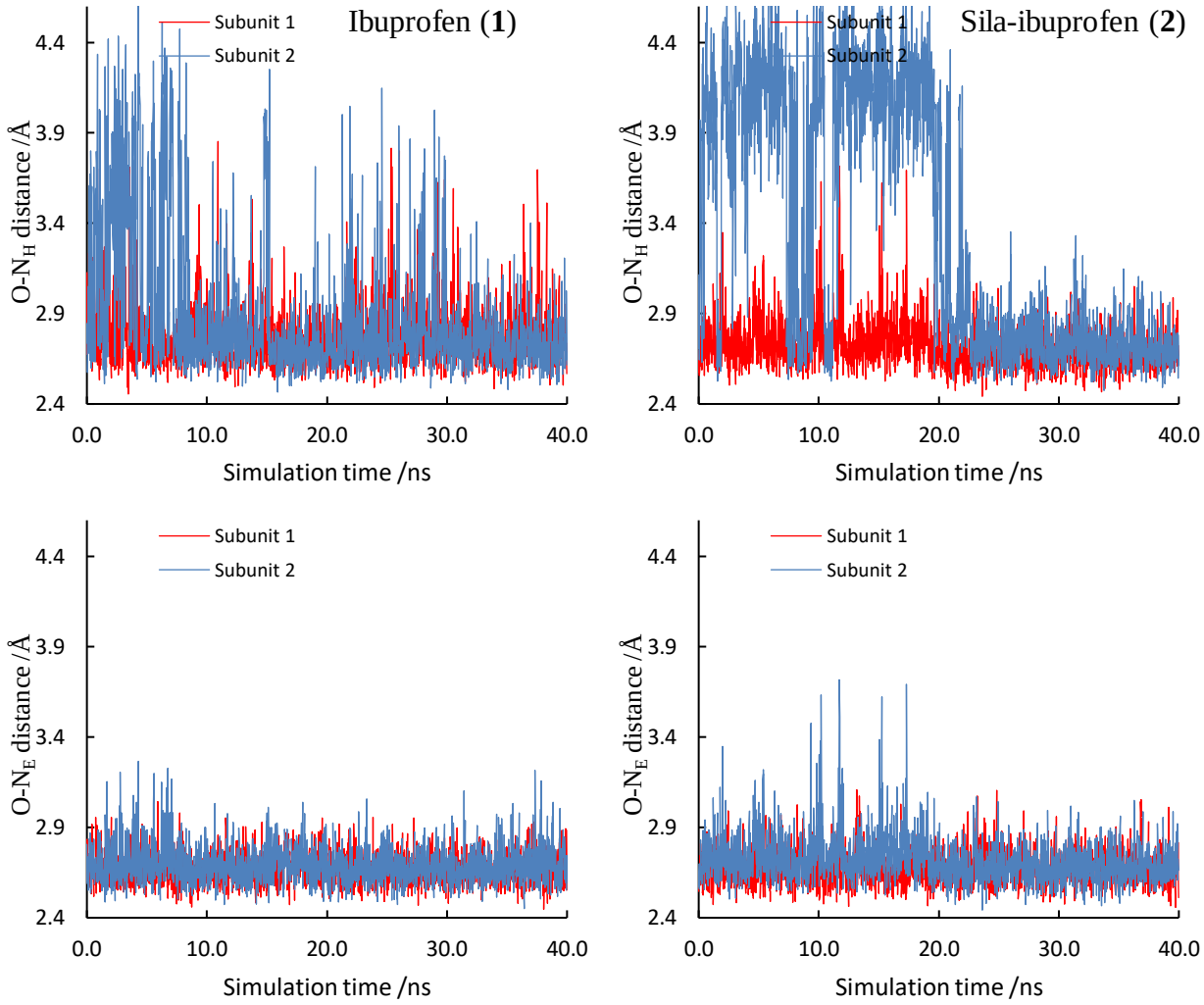

Fig. S16. Plot of arginine-ibuprofen (1,left) and -sila-ibuprofen (2,right) distances for O_1-N_E and O_2-N_H atoms (in force-field nomenclature, structure shown in Figure S7). There are two subunits in COX-I, which are plotted by color-code (red and blue).

4.) Averaged non-covalent interaction index (aNCI)

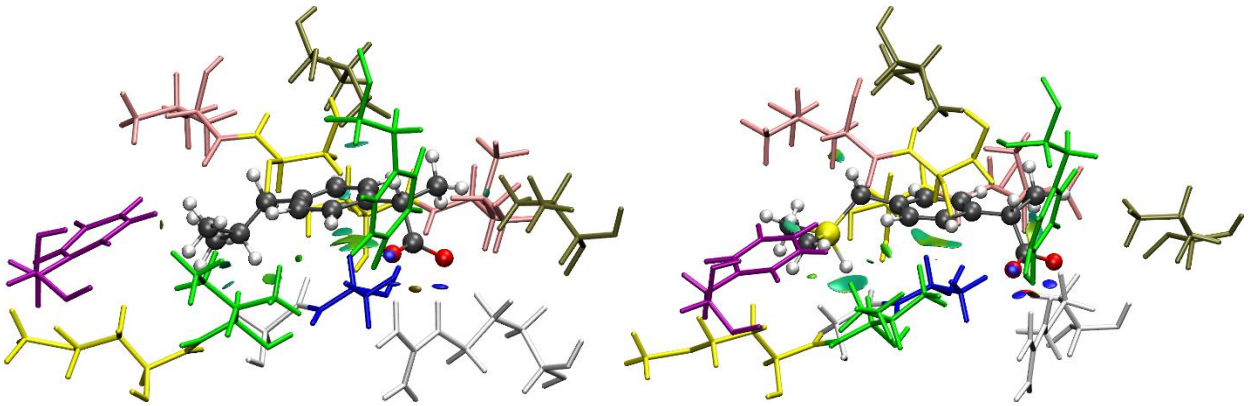

Fig. S17. Visualization of residues important for close interactions inside the active site of COX-I after MD of ibuprofen (**1**,left) and sila-ibuprofen (**2**,right) (color code in Figure 2). Visualization of the aNCI, color code: green = weak dispersion interactions, blue = stronger electrostatic interactions, orange = repulsive interactions.

5.) Averaged interaction energies

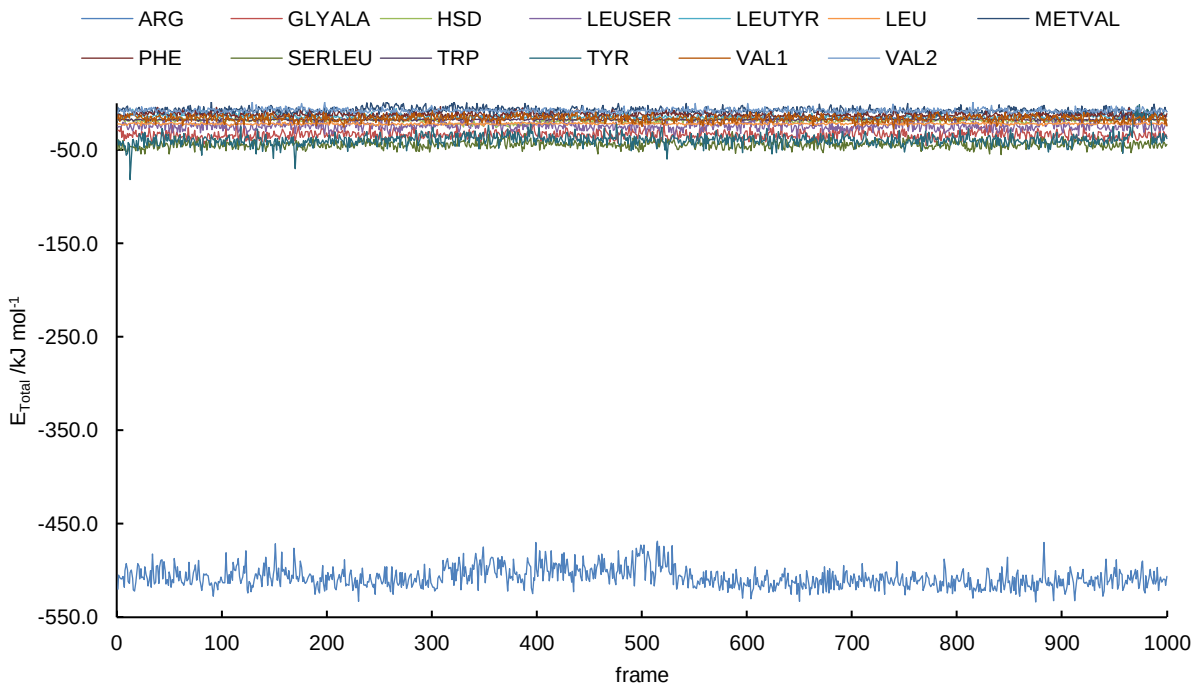

Fig. S18. Plot of total interaction energy over time for sila-ibuprofen (2) in COX-II with 13 residues, which had atoms in a 4 Å radius around atoms of 2.

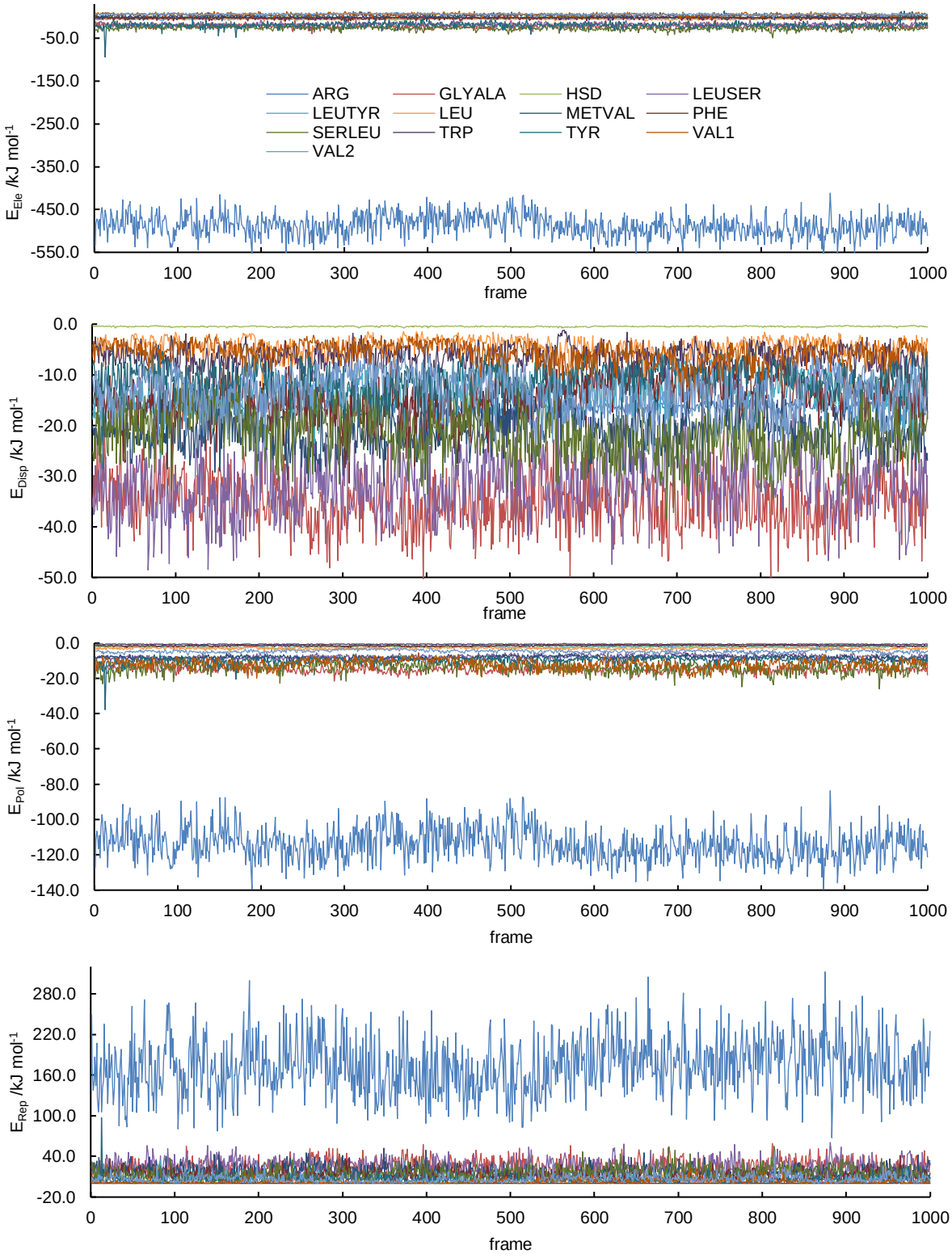

Fig. S19. Plot of interaction energy contributions over time for sila-ibuprofen (2) in COX-II with 13 residues, which had atoms in a 4 Å radius around atoms of 2: electrostatic (top), dispersion (mid, upper), polarization (mid, lower) and exchange repulsion (bottom).

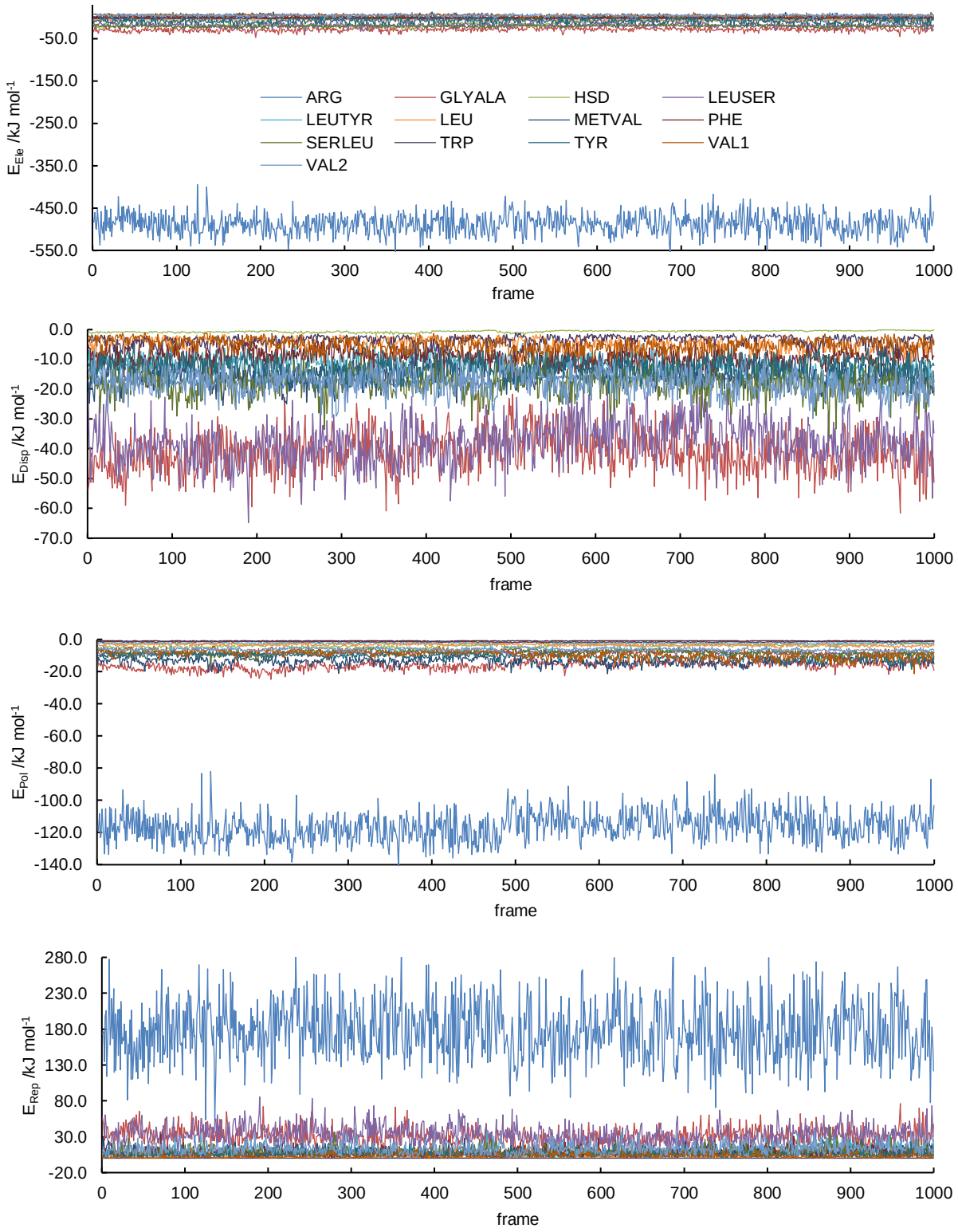

Fig. S20. Plot of interaction energy contribution over time for ibuprofen (1) in COX-II with 13 residues, which had atoms in a 4 Å radius around atoms of 1: electrostatic (top), dispersion (mid, upper), polarization (mid, lower) and exchange repulsion (bottom).

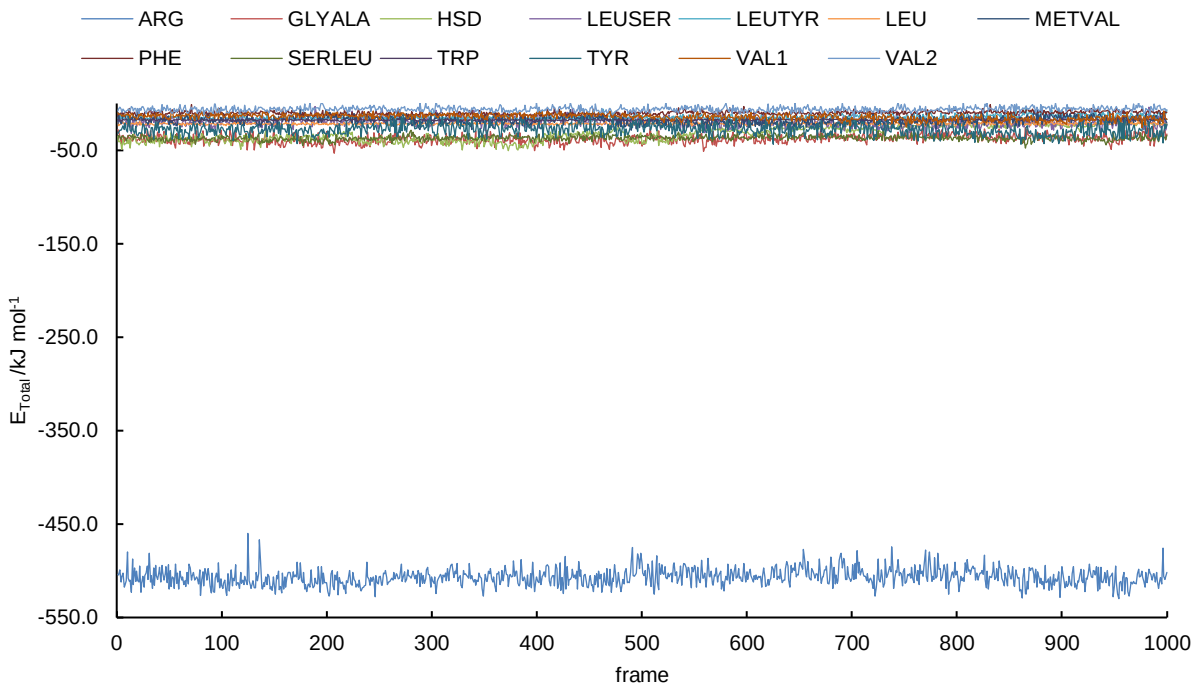

Fig. S21. Plot of total interaction energy over time for ibuprofen (1) in COX-II with 13 residues, which had atoms in a 4 Å radius around atoms of 1.

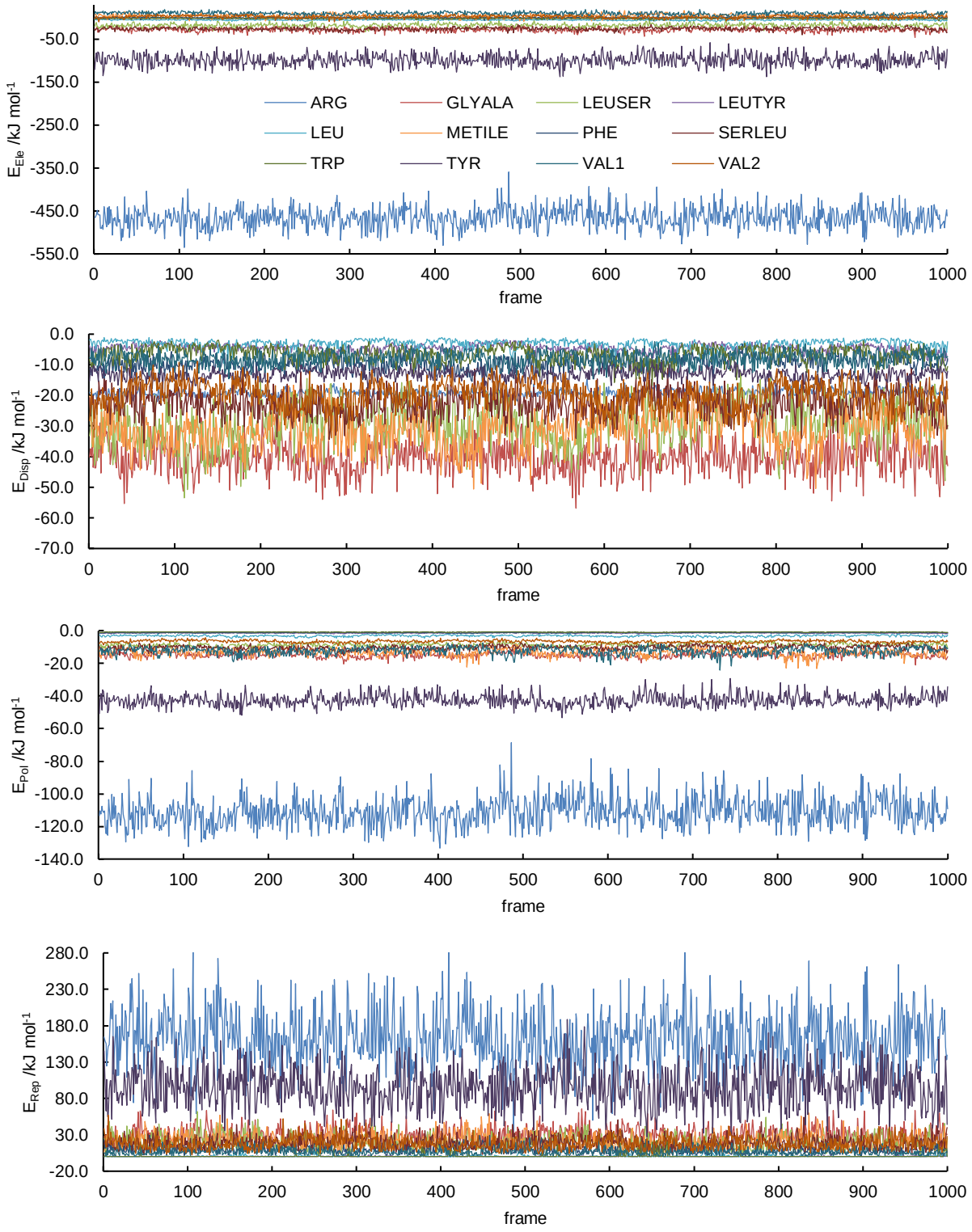

Fig. S22. Plot of interaction energy contributions over time for sila-ibuprofen (**2**) in COX-I with 12 residues, which had atoms in a 4 Å radius around atoms of **2**: electrostatic (top), dispersion (mid, upper), polarization (mid, lower) and exchange repulsion (bottom).

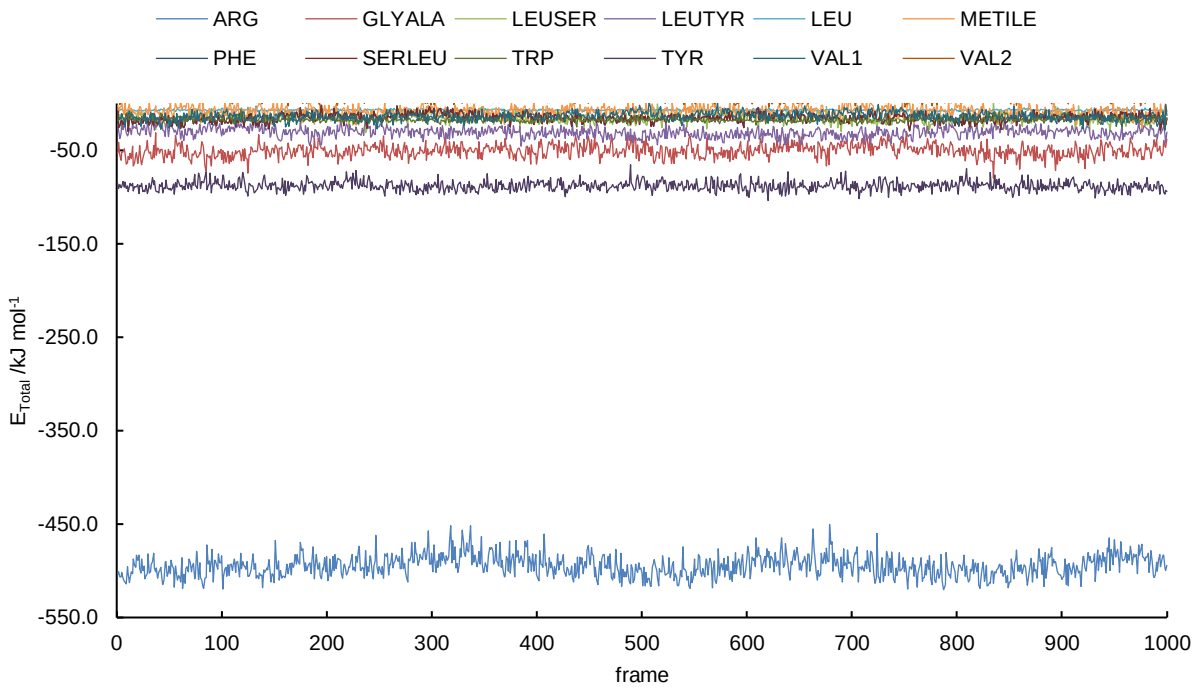

Fig. S23. Plot of total interaction energy over time for sila-ibuprofen (2) in COX-I with 12 residues, which had atoms in a 4 Å radius around atoms of 2.

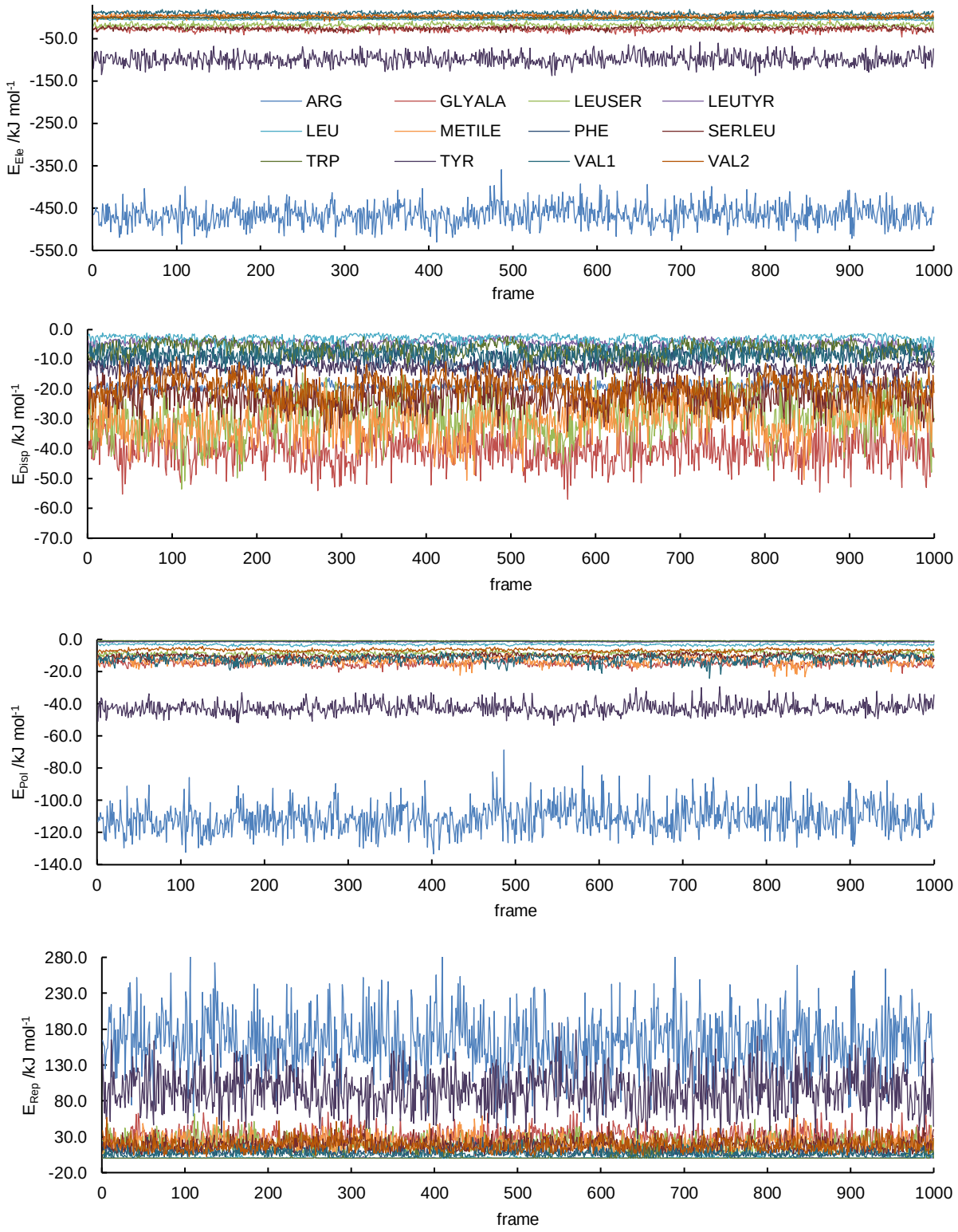

Fig. S24. Plot of interaction energy contributions over time for ibuprofen (**1**) in COX-I with 12 residues, which had atoms in a 4 Å radius around atoms of **1**: electrostatic (top), dispersion (mid, upper), polarization (mid, lower) and exchange repulsion (bottom).

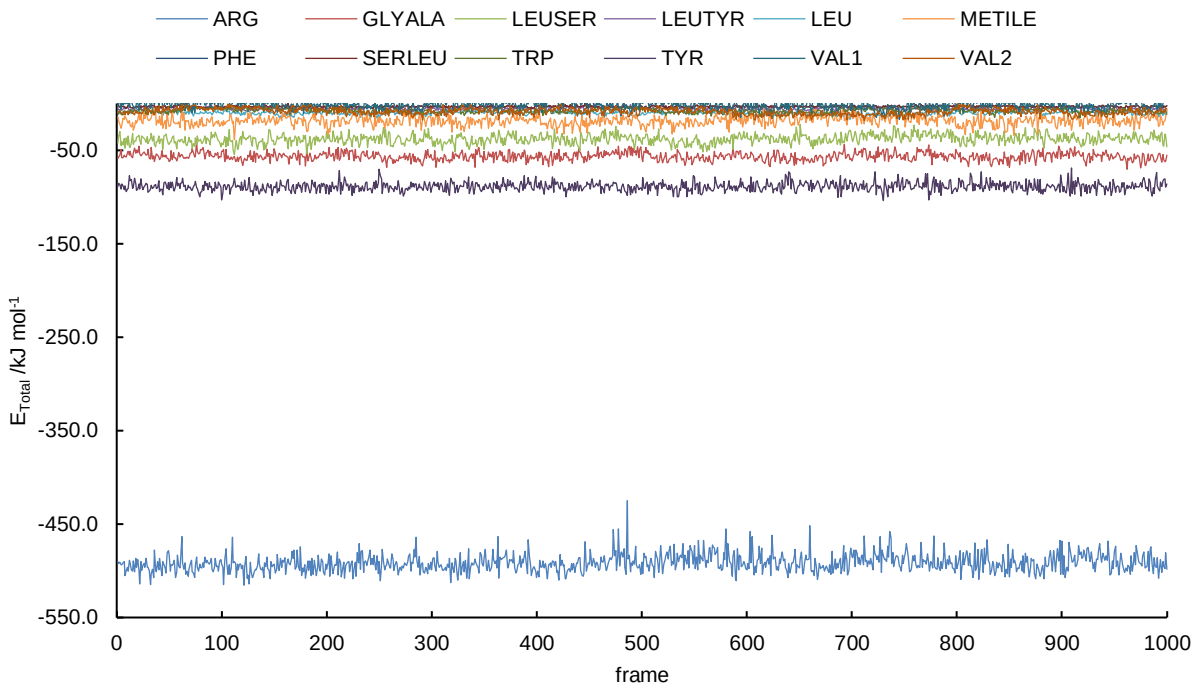

Fig. S25. Plot of total interaction energy over time for ibuprofen (1) in COX-I with 12 residues, which had atoms in a 4 Å radius around atoms of 1.

Table S6.
Full Table of averaged interaction energies in COX-II with estimated standard deviation (ESD) from averaging over trajectories in kJ/mol. Calculated using *tonto*, backend of *CrystalExplorer*.[32]

	Ibuprofen (**1**)					Sila-ibuprofen (**2**)				
Residue	Ele	Disp	Pol	Rep	Total	Ele	Disp	Pol	Rep	Total
Arg	-487(24)	-17.0(10)	-116(9)	178(40)	-508(9)	-487(25)	-16.3(9)	-114(9)	173(41)	-508(11)
GlyAla	-28(4)	-41(6)	-16(2)	31.0(11)	-38(5)	-22(4)	-35(5)	-15.1(15)	26(9)	-34(4)
Hsd	-14(7)	-0.7(3)	-3.8(10)	0(0)	-32(8)	-1.6(18)	-0.41(8)	-2.4(3)	0(0)	-19(2)
LeuSer	-19(5)	-38(7)	-8.2(9)	33(13)	-20(5)	-18(4)	-31(6)	-7.7(11)	25(1)	-24(4)
LeuTyr	-3(2)	-12(3)	-2.4(6)	9(6)	-15(2)	-2.9(17)	-14(3)	-1.7(3)	9(6)	-14(2)
Leu	-5.8(13)	-7(2)	-3.3(6)	3(3)	-21.7(10)	-5.4(11)	-4.4(17)	-3.1(5)	2(2)	-21.9(8)
MetVal	2(4)	-15(3)	-14(2)	8(5)	-18(4)	2(3)	-21(4)	-8.3(10)	18(8)	-8(3)
Phe	0.8(14)	-9(2)	-1.36(15)	8(5)	-10.2(19)	-3(2)	-14(4)	-1.5(3)	12(7)	-12(2)
SerLeu	-20(2)	-18(4)	-8.1(16)	9(6)	-37(3)	-27(4)	-22(5)	-14(3)	16(8)	-44(4)
Trp	-1.9(7)	-3.7(15)	-0.77(12)	0.1(12)	-17.6(8)	-1.7(7)	-6(2)	-0.71(11)	0.1(12)	-17.4(8)
Tyr	-8(5)	-13(3)	-10.4(17)	6(4)	-28(6)	-19(7)	-11(3)	-9.9(18)	6(5)	-39(7)
Val1	5(2)	-5(2)	-9(2)	3(3)	-14(3)	5(3)	-5(2)	-12(3)	3(3)	-16(3)
Val2	5(2)	-18(4)	-6.0(8)	13(7)	-6(3)	6(2)	-13(4)	-4.7(8)	8(5)	-8(2)
Σ	-574(90)	-195(40)	-199(23)	301(103)	-764(50)	-574 (60)	-195(40)	-195(22)	296(105)	-765(45)

Table S7.
Full Table of averaged interaction energies in COX-I with ESD from averaging over trajectories in kJ/mol. Calculated using *tonto*, backend of *CrystalExplorer*.[32]

	Ibuprofen (**1**)					Sila-ibuprofen (**2**)				
Residue	Ele	Disp	Pol	Rep	Total	Ele	Disp	Pol	Rep	Total
Arg	-449(25)	-19.7(16)	-98(9)	134(39)	-494(12)	-465(24)	-19.1(11)	-111(8)	161(39)	-492(10)
GlyAla	-29(4)	-34(4)	-12.0(10)	31(10)	-51(7)	-28(5)	-40(5)	-14.9(15)	30(10)	-57(4)
LeuSer	-16(4)	-35(7)	-7.4(9)	25(11)	-16(5)	-18(4)	-29(7)	-8.6(12)	20(10)	-38(5)
LeuTyr	-1.7(14)	-10(3)	-1.9(4)	4(3)	-31(5)	-0.6(11)	-4.6(12)	-1.34(16)	0.4(5)	-5.4(16)
Leu	-5.4(10)	-4.5(19)	-3.2(5)	2(2)	-7.1(9)	-5.3(9)	-3.3(15)	-3.1(5)	0.7(14)	-10.2(17)
MetVal	-2(5)	-34(6)	-21(3)	27(10)	-9(5)	5(4)	-31(6)	-13(2)	22(9)	-18(5)
Phe	0.1(14)	-9(2)	-1.09(12)	8(5)	-15(4)	-0.1(14)	-10(2)	-1.13(13)	10(5)	-3.3(9)
SerLeu	-24(3)	-23(4)	-6.9(9)	19(8)	-25(4)	-26(3)	-23(4)	-10.3(13)	19(8)	-43(4)
Trp	-1.8(8)	-7(2)	-0.57(7)	0.5(26)	-17(2)	-1.7(8)	-7(2)	-0.74(10)	1(3)	-8(2)
Tyr	-103(15)	-18(2)	-45(4)	98(29)	-88(5)	-99(13)	-13.2(17)	-43(4)	95(27)	-89(5)
Val1	3(3)	-7.3(19)	-12(2)	6(4)	-14(4)	10(4)	-8(2)	-12(2)	7(4)	-1(4)
Val2	6.3(20)	-14(3)	-4.9(7)	8(5)	4(2)	2(3)	-20(4)	-6.5(8)	18(8)	-9(3)
Σ	-622(65)	-216(40)	-213(23)	364(128)	-762(56)	-626(65)	-207(38)	-225(22)	383(125)	-773(47)

6.) Free energy perturbation (FEP) calculations

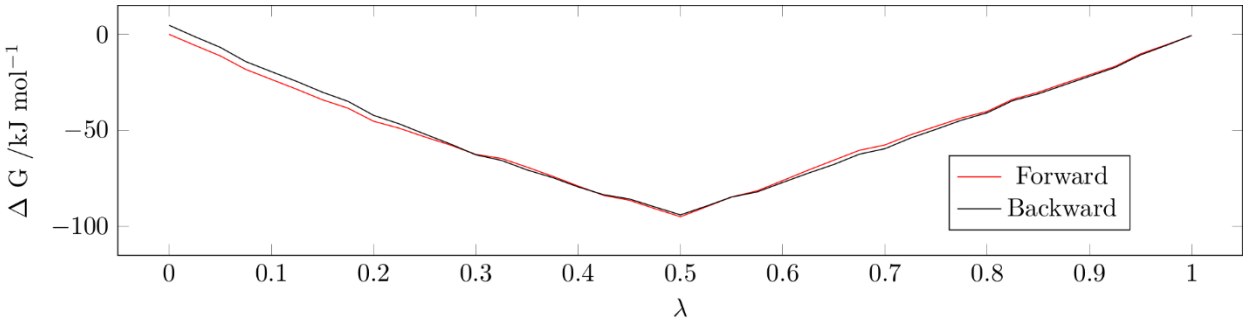

Fig. S26. Plot of ΔG against λ for COX-II, corresponding to the free energy change at each level of perturbation during the simulation.

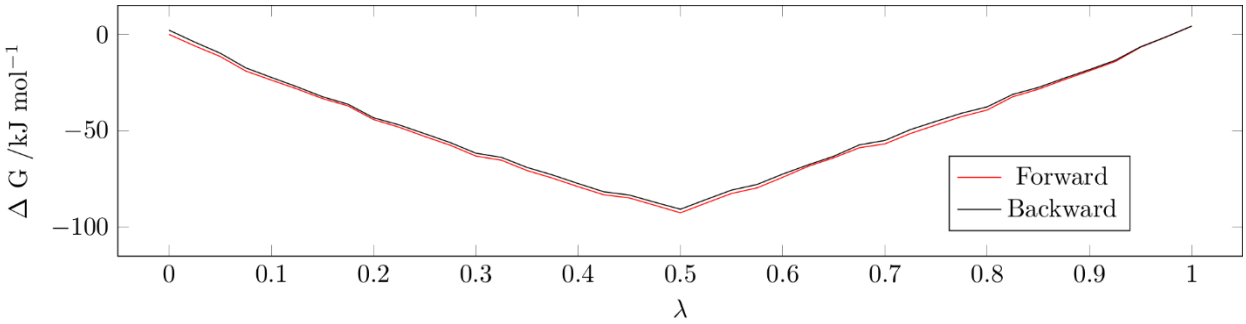

Fig. S27. Plot of ΔG against λ for COX-I, corresponding to the free energy change at each level of perturbation during the simulation. Color code as above.

7.) Toxicological investigations

Cell cultures and experimental incubations

The C6 glioma cell line was purchased from the European Collection of Authenticated Cell Cultures (Lot number: 17A034, passage number: +2). The cells were cultured as recently described in detail.[39] Briefly, the cells were cultured in cell culture medium (90% Dulbecco's modified Eagle's medium (DMEM) containing 25 *mM* glucose, with 10% fetal calf serum (FCS), 44.6 *mM* sodium bicarbonate, 1 *mM* pyruvate, 18 *units/mL* penicillin G and 18 *µg/mL* streptomycin) in 175 cm^2 flasks at 37°*C* with 10% CO_2 in humidified atmosphere in incubators from Sanyo (Osaka, Japan). Cells were subcultured after reaching approximately 80% confluency by washing the cells with 10 *mL* of pre-warmed (37°*C*) phosphate-buffered saline (PBS; 10 *mM* potassium phosphate buffer pH 7.4, 150 *mM* NaCl). Subsequently, cells were detached by incubation in 10 *mL* PBS containing 0.05 % trypsin for 5 *min* at 37°*C* with 10% CO_2. After addition of 10 *mL* cell culture medium the cell suspension was centrifuged for 5 *min* at 400 *g*, the supernatant was aspirated, and the cell pellet was resuspended in 10 *mL* fresh cell culture medium. The cell number in the suspension was determined using a Neubauer counting chamber. For experiments cells were seeded in 1 *mL* cell culture medium into wells of 24-well plates at a density of 50,000 viable cells/well and were used for experiments 24 *h* after seeding.

Cells were then exposed to ibuprofen (**1**) or sila-ibuprofen (**2**) by adding 10 *µL* of a 100-times concentrated stock in ethanol to the cell culture medium to yield final concentrations of up to 1000 *µM* of the substances and 1% ethanol. Cells were subsequently incubated for 24, 48 or 72 *h* at 37°*C* with 10% CO_2. After incubation the cell morphology was examined by phase contrast

microscopy and the incubation media were harvested to determine the extracellular lactate dehydrogenase (LDH) activity as indicator for potential membrane impairment. The cells were washed and treated as described below to determine cellular LDH activity, cellular WST-1 reduction capacity and cellular protein content.

Measurement of LDH activity and protein content

The extra- and intracellular LDH activity was determined as described previously in detail.[40] Briefly, 10 μL of the harvested incubation medium were used for the determination of the extracellular LDH activity. For the determination of the cellular LDH activity the cells were washed twice with 1 *mL* ice-cold (4°*C*) PBS and subsequently lysed with 1% (w/v) Triton X-100 in DMEM for at least 30 *min* at *4°C*. 10 μL of the lysates were used to determine the cellular LDH activity.

For determination of the cellular protein content, the cells were washed twice with 1 mL ice-cold (4°*C*) PBS and the dry cells were stored at -20°C before the protein content of the cells was determined using the Lowry method[40] with bovine serum albumin as a standard protein.

Determination of extracellular lactate and cell-dependent WST1 reduction

The lactate concentration in media samples was determined as described previously.[41] Briefly, media samples harvested after a total incubation time of 72 *h* were diluted 1:5 in pure water. 10 μL of diluted media samples were mixed with 170 μL pure water in wells of a 96-well plate. Subsequently, 180 μL of freshly prepared reaction mixture (5.6 *mM* NAD+, 37.7 *units/mL* LDH, 3.89 *units/mL* glutamate pyruvate transaminase (GPT) in 500 *mM* glutamate/KOH buffer, pH 8.9) were added to each well and the plate was incubated for 90 *min* at 37°*C* in the humidified atmosphere of an incubator and the absorbance at 340 *nm* was measured in a Sunrise microtiter plate spectrophotometer (Tecan, Crailsheim, Germany).

The WST-1 reduction of the C6 glioma cells was determined using a modification of a method described recently in detail.[42] After the incubation the incubation medium was aspirated and the cells were washed twice with 0.5 *mL* pre-warmed (37°C) glucose-free incubation buffer (IB: 20 *mM* HEPES, 145 *mM* NaCl, 5.4 *mM* KCl, 1.8 *mM* $CaCl_2$, 1 *mM* $MgCl_2$, 0.8 *mM* Na_2HPO_4, pH 7.4) and subsequently incubated with 200 μL IB containing 5 *mM* glucose, 400 μM WST-1 and 50 μM menadione. After 30 *min* incubation at 37°*C*, 50 μL of the incubation medium was taken, mixed with 150 μL pure water in wells of a microtiter plate and the absorbance at 405 *nm* was measured in a Sunrise microtiter plate spectrophotometer (Tecan, Crailsheim, Germany).

Materials

Dulbecco's modified Eagle's medium (DMEM) and penicillin/streptomycin solution were purchased from Invitrogen-Gibco (Darmstadt, Germany). Fetal calf serum (FCS), menadione, ethanol and Triton X-100 were obtained from Sigma (Steinheim, Germany). DMSO was obtained from VWR Chemicals (Darmstadt, Germany). Trypsin solution was purchased from Biochrom (Berlin, Germany). WST-1 was obtained from Dojindo (Munich, Germany). 2-[(4-bromomethyl)phenyl]propionic acid and dimethylchlorosilane were obtained from abcr (Karlsruhe, Germany) and ibuprofen (**1**) sodium salt was purchased from Merck (Darmstadt, Germany). The enzymes lactate dehydrogenase (LDH) and glutamate pyruvate transaminase (GPT) were obtained from Roche Diagnostics (Mannheim, Germany)

Other chemicals of the highest purity available were purchased from Merck (Darmstadt, Germany), Applichem (Darmstadt, Germany), Fluka (Buchs, Switzerland), Roth (Karlsruhe,

Germany) or Riedel-de-Haën (Seelze, Germany). Sterile 175 cm^2 flasks were obtained from VWR (Darmstadt, Germany). Sterile 24-well cell culture plates and unsterile 96-well microtiter plates were obtained from Sarstedt (Nümbrecht, Germany).

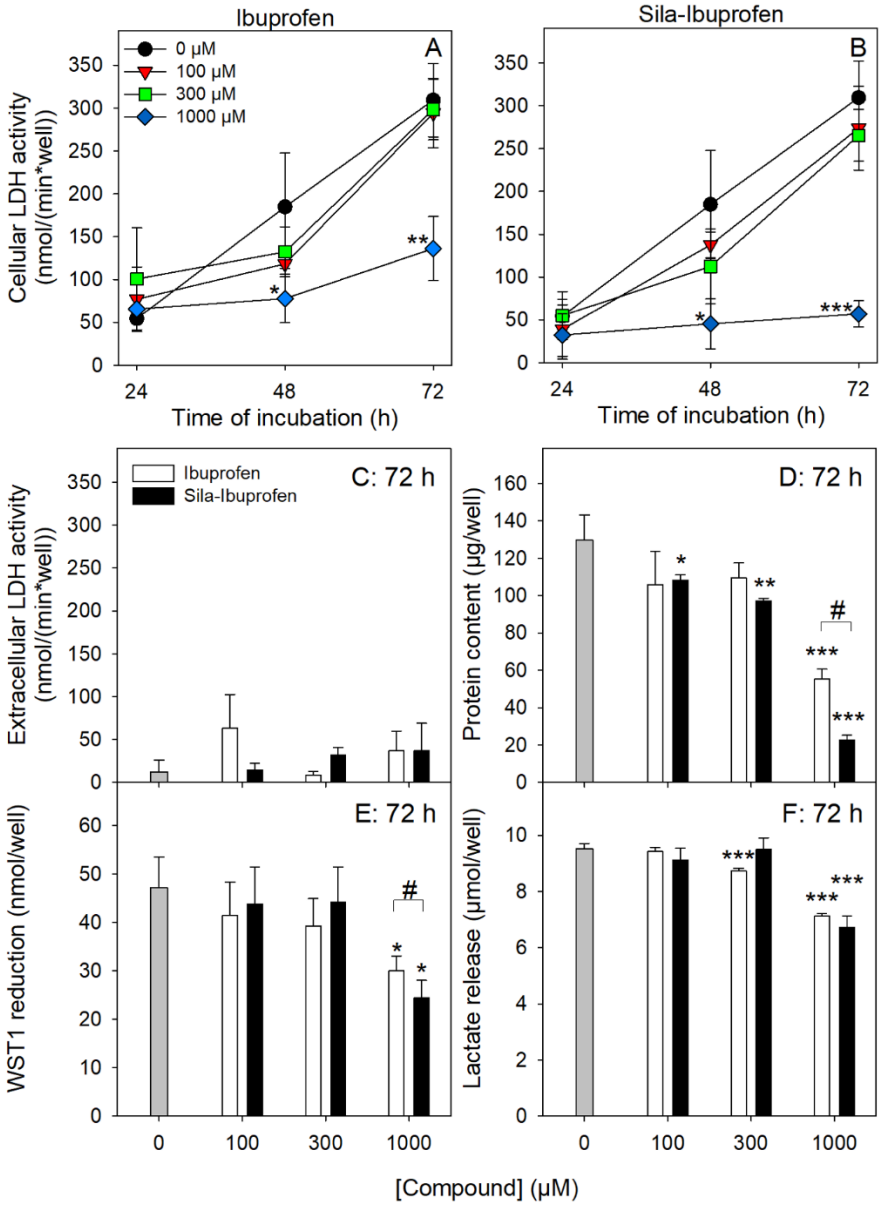

Fig. S28.
Time- and concentration-dependent effects of ibuprofen (**1**) or sila-ibuprofen (**2**) on the viability and metabolic activity of C6 glioma cells. The cells were incubated for up to 72 *h* (A, B) or for 72 *h* (C-F) with **1** or **2** in the concentrations indicated before the cellular (A, B) and extracellular (C) LDH activity, the cellular protein content (D), the cell-dependent WST1 reduction (E) and the lactate release (F) were determined. The data represent means ± SD of values obtained in 3 experiments performed on different passages of C6 cells. Significant differences compared to the control condition (0 μM of the compound) were calculated by ANOVA (followed by the Bonferroni post hoc test) and are indicated by *p<0.05, **p<0.01 and ***p<0.001. Significant differences between the data obtained for incubations with **1** or **2** in a given concentration were calculated by the paired t-test and are indicated by #p<0.05.

8. Enzyme activity measurements to determine IC_{50} values

Table S8.
Inhibition (% of control) of COX-I and COX-II by **1** and **2**, one repetition each

	Ibuprofen (**1**)				Sila-ibuprofen (**2**)			
Concentration /µM	COX-I		COX-II		COX-I		COX-II	
0.1	16.9	11.0	29.3	28.9	19.1	23.1	16.7	16.0
0.316	4.8	7.0	39.8	44.3	26.3	26.5	18.3	23.8
1.0	-0.6	22.9	54.8	53.3	19.0	20.8	34.6	28.3
3.16	5.0	11.1	54.0	57.9	19.5	24.7	47.5	45.8
10	6.4	20.1	68.1	67.6	33.9	35.7	57.2	53.3
31.6	54.7	72.6	85.5	79.6	57.4	64.9	70.6	74.9
100	94.5	88.7	90.6	94.4	78.0	86.0	99.1	91.4

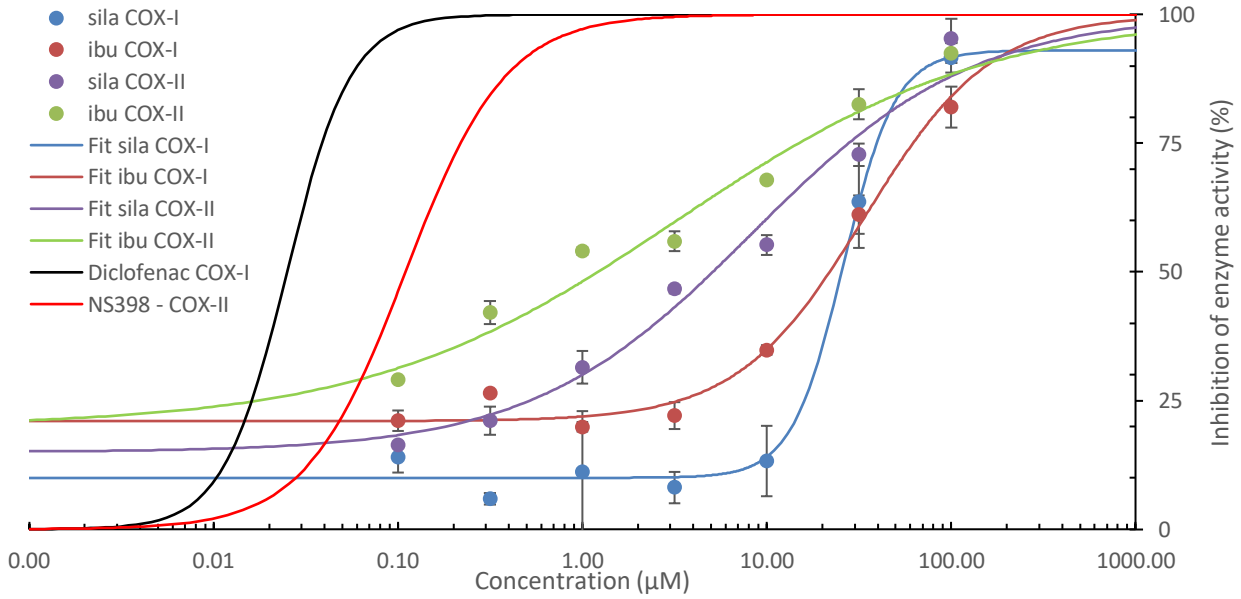

Fig. S29.
Concentration-dependent inhibition of COX-I and COX-II by ibuprofen (**1**, "ibu") and sila-ibuprofen (**2**, "sila"). Shown are also the fitted regression curves for the compounds investigated as well as for the reference substances diclofenac and NS398 used for validation of the test systems.

9. References to methods and software used in the bonding analysis

- Quantum Theory of Atoms in Molecules (QTAIM)[43]: software AIMAll.[44]
- Electron Localizability Indicator (ELI)[45]; Raub-Jansen index[46]: software DGrid-5.0.[47]
- Natural bond orbitals (NBOs) including natural population analysis (NPA) and natural localized molecular orbitals (NLMOs)[48]; natural resonance theory (NRT)[49]: software NBO-7.0.[50]
- Electrostatic potential (ESP) plotted using VMD[51] based on a grid file calculated with cuQCT (home-written software, unpublished).

10. Captions for other Supporting Information

Movie S1.
Guided visual representation of sila-ibuprofen – COX-II complex (ball and stick representation for sila-ibuprofen and NewCartoon[52] for COX-II 0:00 – 0:10), amino acid residues of importance (licorice representation, 0:10 – 0:33) and aNCI isosurfaces (starting from 0:19) with color code; then a side by side comparison of sila-ibuprofen (**2**,left) and ibuprofen (**1**,right) aNCI plots. Representations were created using VMD 1.9.3[51] and the video rendered using Blender 2.79b.[53] Geometries used for the visualization of the atom positions correspond to the last frame of a 1 ns production run, the aNCI is averaged over 1000 frames of this run.

Data S1. (separate file: interaction_energies.xlsx)
Interaction energies for each frame and the analysis of average and wRMSD, separated by contribution (Ele, Disp, Pol and Rep) and in total for sila-ibuprofen and ibuprofen, respectively, as well as a tab with summary for both.

Data S2. (separate file: bond_length_plots.xlsx)
O-N bond lengths in each frame of MD for sila-ibuprofen and ibuprofen, respectively, both subunits.

Data S3. (separate files: bond_order.xlsx)
Bond properties from QTAIM and NBO analysis for all bonds and ELI-D for selected bonds.

Data S4. (separate files: *.cif, *.fcf and *.pdf)
Crystallographic information files (CIFs) of **1** and **2**, including measured reflection intensities and checkcif reports.

Data S5. (separate file: biochemical_data.csv)
Names, SMILES notation and IC_{50} values of ibuprofen **1** and sila-ibuprofen **2**.

11. References for Supporting Information

(38) Mayne, C. G.; Saam, J.; Schulten, K.; Tajkhorshid, E.; Gumbart, J. C. Rapid parameterization of small molecules using the force field toolkit. *J. Comput. Chem.* **2013**, *34*, 2757-2770.
(39) Joshi, A.; Rastedt, W.; Faber, K.; Schultz, A. G.; Bulcke, F.; Dringen, R. Uptake and toxicity of copper oxide nanoparticles in C6 glioma cells. *Neurochem. Res.* **2016**, *41*, 3004.
(40) Lowry, O. H.; Rosebrough, N. J.; Farr, A. L.; Randall, R. J. Protein measurement with the Folin phenol reagent, *J. Biol. Chem.* **1951**, *193*, 265-275.
(41) Tulpule, K.; Hohnholt, M. C.; Hirrlinger, J.; Dringen, R. "Primary cultures of astrocytes and neurons as model systems to study the metabolism and metabolite export from brain cells" in *Brain Energy Metabolism*. Springer, New York **2014,** 45-72.
(42) Stapelfeldt, K.; Ehrke, E.; Steinmeier, J.; Rastedt, W.; Dringen, R. Menadione-mediated WST1 reduction assay for the determination of metabolic activity of cultured neural cells, *Anal. Biochem.* **2017**, 538, 42-52.
(43) Bader, R. F. W. *Atoms in Molecules: A Quantum Theory*, Clarendon Press, Oxford, **1994**.
(44) Keith, T. A., *AIMAll* (Version 19.10.12), TK Gristmill Software, Overland Park KS, USA, **2019** (aim.tkgristmill.com).
(45) Kohout, M. Bonding indicators from electron pair density functionals. *Faraday Discuss* **2007**, *135*, 43-54.
(46) Raub, S.; Jansen, G. A quantitative measure of bond polarity from the electron localization function and the theory of atoms in molecules. *Theor. Chem. Acc.* **2001**, *106*, 223 – 232.
(47) Kohout, M. *DGrid*, Radebeul, Germany **2011**.
(48) Weinhold, F.; Landis, C. R.**;** Glendening, E. D. What is NBO analysis and how is it useful? *Int. Rev. Phys. Chem.* **2016**, *35*, 399-440.
(49) Glendening, E.D.; Landis, C. R.; Weinhold, F. Resonance theory reboot. *J. Am. Chem. Soc.* **2019**, *141*, 4156-4166.
(50) Glendening, E.D.; Badenhoop, J, K.; Reed, A. E.; Carpenter, J. E.; Bohmann, J. A.; Morales, C. M.; Karafiloglou, P.; Landis, C. R.; Weinhold, F. *NBO 7.0*, Theoretical Chemistry Institute, University of Wisconsin, Madison **2018**.
(51) Humphrey, W.; Dalke, A.; Schulten, K. VMD – Visual molecular dynamics. *J. Mol. Graph.* **1996**, *14*, 33-38.
(52) Frishman, D.; Argos, P. Knowledge-based secondary structure assignment. *Proteins: structure, function and genetics* **1995**, *23*, 566-579.
(53) Blender Online Community, Blender – a 3D modelling and rendering package (blender.org).